



The Rowley Shoals atolls: Remnants of a Miocene great barrier reef on the north-west Australian margin

Jackson C. McCaffrey^a, Stephen J. Gallagher^{a,*}, Malcolm W. Wallace^a, Tanita Averes^b, Stanislaus G. Fabian^a, Katja Lindhorst^b, Lars Reuning^b, Sebastian Krastel^b

^a School of Geography, Earth and Atmospheric Sciences, The University of Melbourne, Parkville, Victoria 3010, Australia

^b Institute of Geosciences, Kiel University, Kiel 24118, Germany

ARTICLE INFO

Editor: Liviu Matenco

Keywords:

Miocene
Atoll reefs
Northwest Shelf of Australia
Rowley Shoals
Seismic stratigraphy

ABSTRACT

The tropical North West Shelf of Australia hosts a diverse range of modern reefs. Six shelf edge isolated atolls are present north of 18°S including: Ashmore Reef, Scott Reef and Seringapatam Reef, and three Rowley Shoals. The Ningaloo Reef is a fringing reef around the North West Cape at 22°S. All of these reefs are the remnants of a vast 2000 km long barrier reef that drowned during the Late Miocene (~10 Ma). Despite extensive hydrocarbon exploration in the region, the history of these isolated reefs is not well known. Seismic analyses combined with stratigraphic analyses of International Ocean Discovery Site U1464 near the Rowley Shoals has revealed that these modern isolated atolls have a complex evolution related to climate and tectonism as they managed to survive on their Miocene barrier reef foundation.

The first Miocene reefs (~17 Ma) near the Rowley Shoals were isolated small, mound-shaped features. These evolved into a barrier reef by the Middle Miocene (~16 Ma). However, by the Late Miocene (~10 Ma) this barrier reef backstepped landward, evolved into isolated mounds/atolls and drowned prior to the Miocene-Pliocene boundary (~6 Ma) largely due regional tectonic subsidence. Early Pliocene reef expansion (~4.6 Ma) led to the growth of four isolated atolls (the Rowley Shoals) related to local faulting and Early Pliocene warmth. Subsequently a second Pliocene reef growth phase occurred from ~3.5 to 3 Ma when eastern Indian Ocean sea surface temperatures cooled by ~4 °C due to Indonesian Gateway constriction and a reduced Leeuwin Current. By the Pleistocene (~2.4 Ma) one the four Rowley Shoals had drowned. Strong sea level variability, together with Indonesian Throughflow constriction and reduction in intensity of the Leeuwin Current after 2.4 Ma may have led to enhanced cooling and regional upwelling. These factors may have been sufficient to cause local drowning of the southerly fourth Rowley Shoal while the more northerly three Shoals survived until present.

1. Introduction

The north-west margin of Australia hosts a range of modern reefal carbonate systems such as shelf edge atolls (Ashmore Reef, Scott and Seringapatam Reefs, and the Rowley Shoals) and the North West Cape fringing Ningaloo Reef at 22°S (Fig. 1). Reefs systems like these represent critically important ecosystems on Earth (Wilson et al., 2010; Coker et al., 2014; Edgar et al., 2014). Understanding how they develop over time due to factors such as climate, sea level and oceanographic variability can give us insights into how these and reefs globally may react to similar changes in the future (Kleypas et al., 2001; Bellwood et al., 2004; Woodroffe and Webster, 2014; Hughes et al., 2017). Research into the

geological evolution of these reefs can therefore provide insights into the changes these reefs have undergone and the factors influencing these changes (cf. Jones et al., 2022; Petrick et al., 2024a).

Historically, research on the sedimentary basins underpinning the modern reefs of the Australian North West Shelf has predominantly focused on the extensive oil and gas deposits and their associated strata (Cretaceous and older), resulting in less emphasis on the overlying Cenozoic sediments, which are not hydrocarbon prospective or targets for hydrocarbon exploration. Previous studies using these datasets to investigate the relationship between the modern reefs and their foundations (e.g., Collins, 2002; Ryan et al., 2009 for the Rowley Shoals; Rosleff-Soerensen et al., 2016 on the nearby Scott Reef) have advanced

* Corresponding author.

E-mail address: sjgall@unimelb.edu.au (S.J. Gallagher).

<https://doi.org/10.1016/j.gloplacha.2024.104688>

Received 6 May 2024; Received in revised form 18 December 2024; Accepted 20 December 2024

Available online 22 December 2024

0921-8181/© 2024 The Authors. Published by Elsevier B.V. This is an open access article under the CC BY license (<http://creativecommons.org/licenses/by/4.0/>).

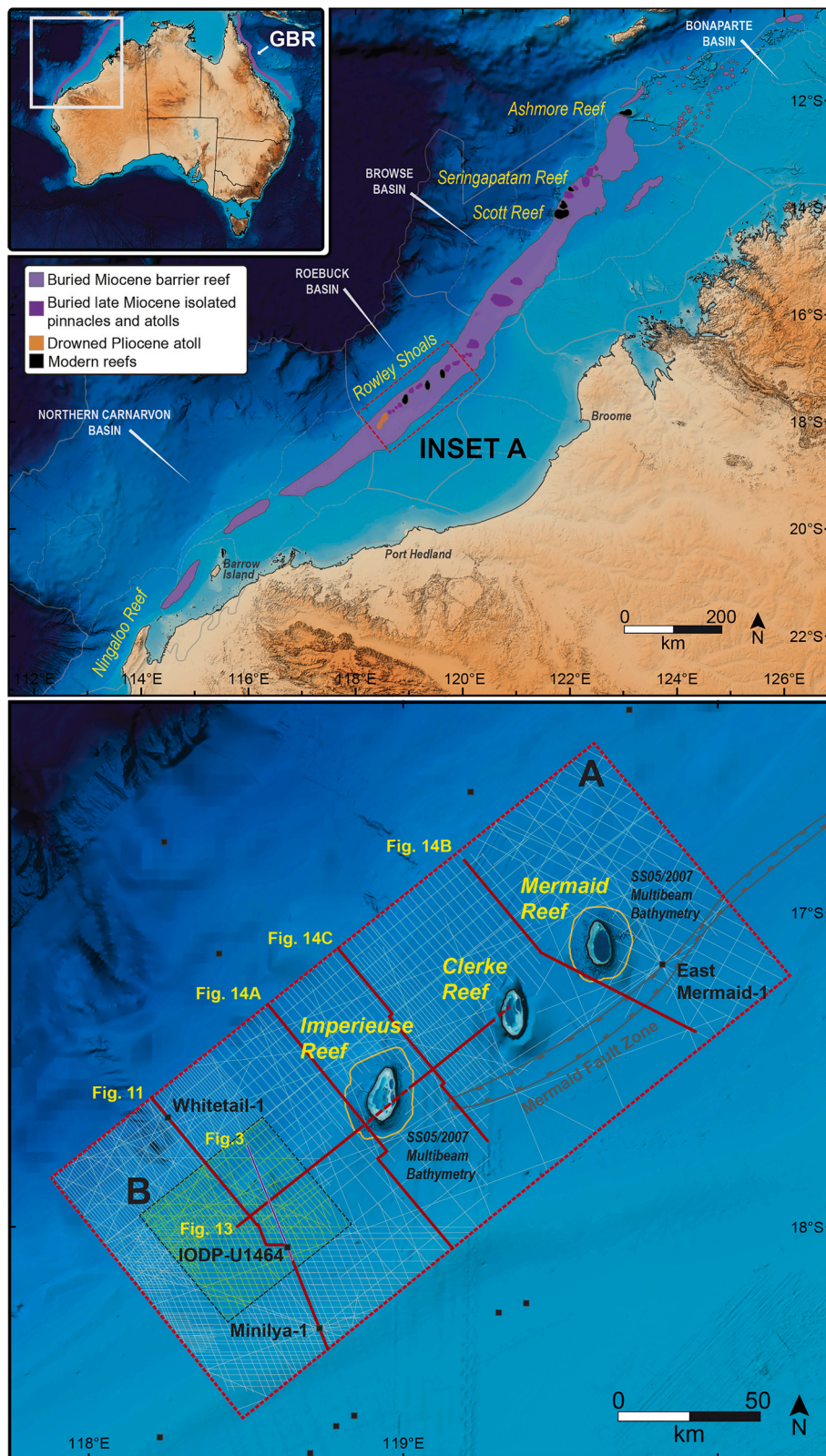


Fig. 1. Map of Northwest Australia. The area in light purple shows the full extent of the Middle Miocene barrier reef complex (McCaffrey et al., 2020). Late Miocene atolls are dark purple. Modern day isolated atolls are shown in black with the drowned Pliocene atoll described in this work orange. A comparison to the size of the modern Great Barrier Reef (GBR) is shown. Insets A and B are the focus areas of this paper in the Rowley Shoals region. 2D Seismic lines used to interpret Rowley Shoals setting are grey. Seismic lines used in drowned Rowley Shoal interpretation area are green. High resolution multibeam bathymetry surrounding Mermaid and Imperieuse Reefs (orange border) was collected on Southern Surveyor Voyage SS05/2007 by the Marine National Facility. The extent of the Mermaid Fault Zone is after Smith et al. (1999). All other bathymetric data are from Australian Topographic and Bathymetric Grid (2009). Aerial images of Rowley Shoals overlain on bathymetry data courtesy of the Earth Science and Remote Sensing Unit, NASA Johnson Space Center (<https://eol.jsc.nasa.gov>; last accessed November 11, 2022). (For interpretation of the references to colour in this figure legend, the reader is referred to the web version of this article.)

our understanding of how these reefs have developed. For instance, Collins (2002) outlines the geological controls on the Quaternary evolution of the Ningaloo Reef, the Rowley Shoals, and Scott Reef. Ryan et al. (2009) explore hypotheses for the Neogene initiation of reefs at the Rowley Shoals, emphasising structural reactivation of the Mermaid Fault Zone and the potential influence of hydrocarbon seepage on reef initiation. Ryan et al. (2009) provided detailed insights into the geological context and morphology of the Rowley Shoals reefs, uncovering their resilience and structural influences from the Middle Miocene. Similarly, Rosleff-Soerensen et al. (2016) documented the development of a continuous Miocene barrier reef in the Browse Basin. The lateral extent of this Miocene barrier reef on the North West margin of Australia was found by McCaffrey et al. (2020) to be over 2000 km long stretching from Cape Range in the southwest to the Timor Sea in the northeast (Fig. 1). This is similar in magnitude to the modern Great Barrier Reef, Queensland, Australia. McCaffrey et al. (2020) suggested that the main controls on the evolution, growth, and demise of the reef system were subsidence, global eustasy, climate variability, and antecedent topography.

We present here the first comprehensive analysis of the Miocene to Recent evolution of the Rowley Shoals reef complex, a series of three ring-shaped isolated atolls located approximately 300 km offshore from the township of Broome, Western Australia (Fig. 1). These atolls reach the sea-surface from approximately 250 m of water depth, with their foundations built upon the central region of the buried Miocene barrier reef system (Collins, 2002; McCaffrey et al., 2020). A fourth, drowned shoal, with similar size and morphology to the other three atolls, is present ~60 km southwest of the Rowley Shoals as revealed in bathymetric data (as a seafloor expression; Jones, 1973), and 2D seismic profiles (Ryan et al., 2009). Previous studies on Rowley Shoals reef evolution (e.g., Collins, 2002; Ryan et al., 2009) were limited by either the availability of data or the scope of the study (usually at basin or sub-basin scale) and were often limited by a lack of age controls available from industry wells. We overcome these limitations by integrating three key new datasets: high-resolution multichannel seismic data from R/V Sonne Expedition 257 (Kuhnt et al., 2018), an extensive grid of over 350 2D seismic profiles from 13 industry surveys, and downhole, core and updated biostratigraphic data from the International Ocean Discovery Program (IODP) Expedition 356 (Gallagher et al., 2017a). This combination of datasets allows us, for the first time, to reveal previously unknown phases of Pliocene reef development, document for the first time the complete morphology of the drowned fourth Rowley Shoal through detailed two-way time (TWT) structure mapping, and establish how regional tectonic subsidence, changes in climate, and oceanographic evolution controlled the complex history of reef growth and drowning in this area.

2. Geological background

The North West Shelf of Australia is a passive continental margin from 10°S to 22°S latitude. It is subdivided into four sedimentary basins: the Northern Carnarvon, Roebuck, Browse and Bonaparte Basins (Fig. 1; Keep et al., 2018; Purcell and Longley, 2023). Oligocene to Miocene strata of the North West Shelf are primarily carbonate that preserve a series of large prograding clinoforms (Mandu and Trealla formations of the Northern Carnarvon Basin and northward lateral equivalents; Heath and Apthorpe, 1984; Apthorpe, 1988). These carbonates are primarily skeletal and include foraminifera, bryozoans, molluscs and corals, in a heterozoan assemblage (Wallace et al., 2003; Cathro et al., 2003; Moss et al., 2004). The sequence stratigraphic framework of the Paleogene to Neogene clinoform sequences have been previously described (Heath and Apthorpe, 1984; Apthorpe, 1988; Hull et al., 1998; Young et al., 2001; Hull and Griffiths, 2002; Cathro et al., 2003; Moss et al., 2004). The clinoforms of the Mandu and Trealla formation have been intensively researched (Heath and Apthorpe, 1984; Apthorpe, 1988; Hull et al., 1998; Young et al., 2001; Hull and Griffiths, 2002; Cathro et al.,

2003; Moss et al., 2004; Cathro and Karner, 2006; Prélat et al., 2015; Rankey, 2017; Tesch et al., 2018; Anell and Wallace, 2020; Riera et al., 2022).

Overlying the progradational sequence, the open shelf Late Miocene to Holocene Delambre Formation has an aggradational or retrogradational stratigraphic geometry (Czarnota et al., 2013). In the southern North West Shelf (Northern Carnarvon Basin), Late Miocene to Quaternary Bare Formation siliciclastics and carbonates (Heath and Apthorpe, 1984; Wallace et al., 2003; Cathro et al., 2003; Sanchez et al., 2012; Tagliaro et al., 2018) are interbedded with the Delambre Formation (Sanchez et al., 2012; Tagliaro et al., 2018).

On the north-western margin of Australia, Paleogene to Neogene records of climate variability are influenced by global trends (De Vleeschouwer et al., 2017). Regional climate conditions also appear to be influenced by progressive oceanographic changes driving shifts in precipitation and changes between dry and humid climate conditions (Christensen et al., 2017; Groeneveld et al., 2017). Uplift of the Indonesian Archipelago to the north of Australia, from 10 to 4.4 Ma changed regional oceanographic conditions by trapping warm waters in the central Pacific, forming the Indo-Pacific Warm Pool north of Papua New Guinea. Intermittent connectivity between the Indo-Pacific Warm Pool and the Indian Ocean via the Indonesian Seaway occurred between 1.6 and 0.8 Ma and led to the establishment of the south-flowing Leeuwin Current along the Western Australian coast (Gallagher et al., 2009, 2014, 2024).

Modern global tropical reef distribution is strongly controlled by the presence of these warm currents, such as the East Australian Current (Great Barrier Reef) and Kuroshio Current (Ryukyu Reefs, Japan; Gallagher et al., 2014). Along the western margin of Australia the modern Leeuwin Current transports warm, low salinity, nutrient-deficient water southwards, extending tropical reef development to 30°S off Western Australia (Gallagher et al., 2009; Pattiaratchi, 2006).

3. Cenozoic and modern reefs on the Northwest Shelf

Cenozoic reef development on the North West Shelf of Australia has been summarised by McCaffrey et al. (2020) who described the evolution and demise of a 2000 km long middle Miocene barrier reef (Fig. 1). This drowned reef stretched from the Bonaparte Basin in the northeast (Gorter et al., 2002; Courgeon et al., 2016; Saqab and Bourget, 2016), the Browse Basin (Rosleff-Soerensen et al., 2012, 2016; Belde et al., 2017; Van Tuyl et al., 2018a, 2018b; Thronberens et al., 2022; Williams et al., 2023), the Roebuck Basin (Ryan et al., 2009) and the Northern Carnarvon Basin (Young et al., 2001; Romine et al., 1997; Cathro et al., 2003; Riera et al., 2023) to the southwest. This reef expanded to its maximum extent during the Middle Miocene Climate Optimum. Late Miocene subsidence and climate cooling probably caused its demise leading to less extensive remnants of isolated atolls and pinnacle reefs on the modern shelf (McCaffrey et al., 2020).

The present North West Shelf is a tropical ramp with a variety of coral reefs, ranging from fringing reefs to isolated atoll reefs which rise from deep-ramp settings (Collins, 2002). The modern coral reefs of the North West Shelf include island-related shelf reefs of the Kimberley coast, the Pilbara reefs (Barrow and Montebello Islands), the North West Cape fringing Ningaloo Reef (Fig. 1), and the isolated oceanic reefs of the Bonaparte, Browse and Roebuck Basins (Ashmore Reef, Seringapatam and Scott Reefs, and Rowley Shoals; Fig. 1).

Situated approximately 300 km offshore from Broome, Western Australia, the Rowley Shoals (comprising Mermaid, Clerke, and Imperieuse Reefs; Fig. 1) are a series of emergent annular atoll reefs that rise from a depth of over 230 m from the distal ramp of the seafloor (Fairbridge, 1950; Collins, 2002). The reefs, first described morphologically from LANDSAT images and diver traverses by Berry and Marsh (1986), have similar dimensions, shape and orientation, and are spaced at approximately 30kms between Mermaid and Clerke Reefs and 40kms between Clerke and Imperieuse Reefs.

The three atolls are aligned SW-NE, parallel to the shelf edge. However, individually the reefs have a north-south orientation. They are 7 to 9 km wide, 15 to 17 km long and become narrower towards the northern end. Mermaid Reef encloses a single, relatively deep (20 m) ovoid shaped lagoon, with lagoon depth decreasing (<10 m) and segmentation increasing in Clerke and Imperieuse Reefs (Collins, 2002). The presence of a fourth drowned shoal, 40-50 km SW of Imperieuse Reef, was first described by Jones (1973), and was later verified by Collins (2002) on Precision Depth Recorder (PDR) bathymetry from CSIRO research vessel RV *Franklin* cruise FR05/00 and Ryan et al. (2009) on 2D seismic lines JN87-07 and JN87-08 (Fig. 1).

4. Materials and methods

This study is partly based on the analysis of industrial 2D seismic data, acquired for hydrocarbon exploration along the present-day shelf margin in the Rowley Shoals area of the North West Shelf (Fig. 1). The seismic data is zero phase and follows the SEG European polarity convention (an increase in acoustic impedance correlates to a negative polarity). A bulk-shift in the seismic datum of each survey was also applied in order to make stronger correlations between surveys. This shift was determined based on tying the seafloor horizon of a seismic line to the measured seafloor depth in well data. The seismic data was initially calibrated by petroleum industry wells (Minilya-1 and East

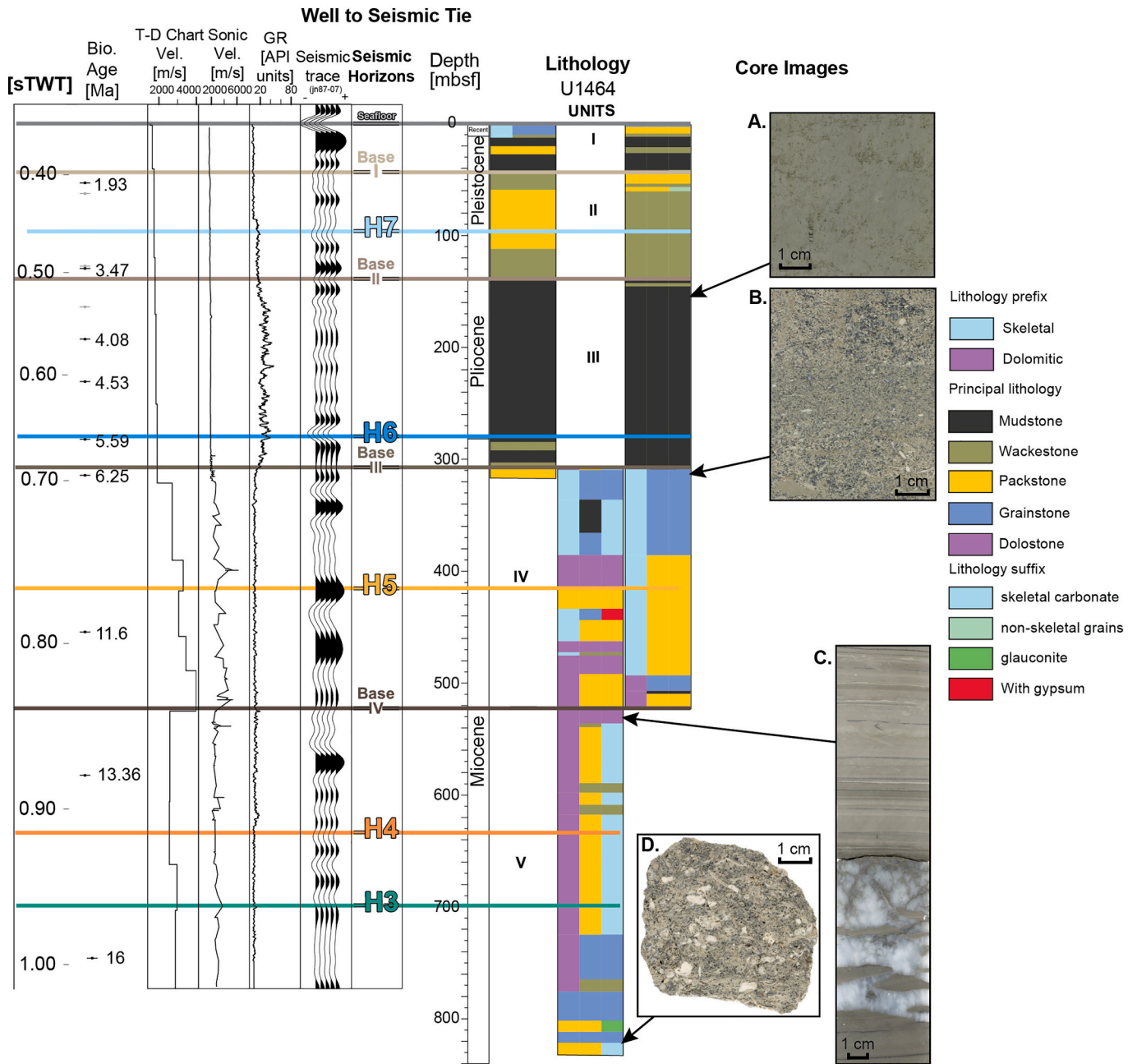


Fig. 2. Seismic stratigraphy and facies of IODP Site U1464 with examples of core images (adapted from Gallagher et al., 2017b and McCaffrey et al., 2020). A. Unlithified greyish green to greenish grey homogeneous mudstone B. Lithified dark greenish grey grainstone with coarse sand-size grains and macrofossils C. Lithified thinly bedded beige to grey dolostone with anhydrite crystals D. Lithified light greenish grey medium sand-sized packstone with abundant bryozoans and bivalve fragments. Well to Seismic ties are shown. Location of Site U1464 is shown on Fig. 1. sTWT = Two Way travel time in seconds, Bio. = Biostratigraphic age, Vel. = velocity, m/s = metres per second, GR = gamma ray log, mbsf = metres below sea floor. (For interpretation of the references to colour in this figure legend, the reader is referred to the web version of this article.)

Mermaid-1), using velocity (check-shot) and biostratigraphic data obtained from well completion reports (McCaffrey et al., 2020). Data from IODP Site U1464 (Fig. 2; Gallagher et al., 2017b) was also used. In the absence of check-shot data, velocity at Site U1464 is calculated by using measured p-wave velocity (caliper values down core). Seismic stratigraphic analysis was conducted on IHS Markit Kingdom software which allowed identification of the main seismic unconformities and their associated seismic sequences. Seismic facies were identified and interpreted on seismic data using the identification criteria of Mitchum Jr. et al. (1977), with carbonate buildups and reef facies interpreted using the identification criteria of Burgess et al. (2013).

Detailed interpretation of the seismic stratigraphy was guided by downhole and core data from International Ocean Discovery Program (IODP) Expedition 356 (Fig. 2; Gallagher et al., 2017a, b) and high resolution seismic acquired from R/V Sonne Expedition 257 (Kuhnt et al., 2018). During this expedition, a Geometrics GeoEel streamer consisting of four solid state sections (32 channels) and a standard 1.7 L GI-gun was deployed across designated sections of the cruise to acquire high resolution 2D multichannel seismic data (Kuhnt et al., 2018). In contrast to the industrial seismic surveys, the acquisition method for this survey was designed to target the upper 500–1000 m of strata (losing fidelity at 1000 m +), while maintaining a high vertical resolution. This dataset therefore has a higher vertical resolution than the industry seismic (~1 m vertical resolution) and has increased seafloor penetration when compared to the sub-bottom profile data.

5. Stratigraphy of the Rowley Shoals

Previous studies of the history of the Miocene reefs and carbonate buildups in the Rowley Shoals region were restricted by limited age controls provided by either seismic correlation to the nearby industry wells (Table 1, Fig. 1) or interpreted stratigraphic horizons from Geoscience Australia’s regional seismic surveys (Australian Geological Survey Organisation, 2001; see Ryan et al., 2009). International Ocean Discovery Program (IODP) Expedition 356 (Indonesian Throughflow, September 2015; Gallagher et al., 2017a,b) cored Site U1464, in the Rowley Sub-basin (Roebuck Basin) (Fig. 1) provided a detailed biostratigraphic framework that can be used to correlate the Middle Miocene to Recent strata of the Rowley Shoals. In particular, IODP Site U1464 is 10 km landward from the fourth, drowned Rowley Shoal and therefore provides an important link in the understanding of the evolution of the modern and drowned Rowley Shoals.

IODP Site U1464 is the only site to core the upper 500 m of strata in the region. It has been divided into five units (Fig. 2, Gallagher et al., 2017b), the first three of which (Units I-III) are unlithified and range from mudstone and skeletal grainstone with peloids (Unit I, 0–44 m below sea floor), homogeneous wackestone and packstone (Unit II, 44–94 m), and mudstone (Unit III, 170–215 m). Units IV and V are lithified dolomitic packstones/limestones, and dolostone with gypsum and anhydrite nodules. Unit IV (215–311 m) yields abundant macrofossils, including reef-building zooxanthellate corals and crustose coralline algae. Unit V (>311 m) is defined by the presence of shelfal deposits near the top of the unit and increasingly coarser packstones and

Table 1
List of wells and cores near the Rowley Shoals (see also Fig. 1).

Site	IODP Exp. 356	Industry well	Latitude	Longitude	Present-day water depth (m)
Minilya-1		X	18°19.40'S	118°44.02'E	146
IODP-U1464	X		18°03.92'S	118°37.89'E	264
Whitetail-1		X	17°39.13'S	118°15.10'E	953
East Mermaid-1		X	17°09.92'S	119°49.41'E	388

grainstones towards its base (Fig. 2).

The age framework for IODP Site U1464 is determined by diagnostic planktic foraminifera (PF), calcareous nannofossils (CN), and larger benthic foraminifera (LBF) (Table 2; Gallagher et al., 2017b; Groeneveld et al., 2017, 2021). The oldest datum at IODP Site U1464 is the first occurrence of the LBF *Nephrolepidina ferreroi*, dated at ~16 Ma (Groeneveld et al., 2017). The upper occurrence of *N. ferreroi* at Site U1464 was impacted by the shallow environmental conditions in the younger strata, and therefore is not interpreted as a stratigraphical event (Groeneveld et al., 2017). The other LBF biostratigraphic datum determined at Site U1464 was the last occurrence of *Flosculinella* spp., at 11.6 Ma (Groeneveld et al., 2017). The shallower environments of Units IV and V also preserve calcareous nannofossils, with the last occurrences of *Discoaster quinqueramus* (5.59 Ma) and *Reticulofenestra rotaria* (6.25 Ma), and the presence of *Calcidiscus macintyreii* indicating a maximum age of 13.36 Ma at 844.2 mbsl (Gallagher et al., 2017b; Groeneveld et al., 2021).

The abundance of planktic foraminifera (PF) increases as the strata transitions to deeper water environments in Unit III at Site U1464, with Units II and I yielding well preserved PF (Gallagher et al., 2017b). As such, biostratigraphic datums from samples in these Units are well constrained (Table 1; Gallagher et al., 2017b, Groeneveld et al., 2021).

6. Seismic stratigraphy

The 2D seismic profile JN87–07 was used by Ryan et al. (2009) to

Table 2
Biostratigraphic datums at IODP Site U1464 (Gallagher et al., 2017b; Groeneveld et al., 2017, 2021), with corresponding lithostratigraphic units and relative positions of seismic horizons H3 to H7 (see Fig. 2). Age types include: Planktic Foraminifera (PF), Calcareous Nannofossils (CN), and Larger Benthic Foraminifera (LBF).

Unit	Age Datum/ Stratigraphic Event	Age Type	Age [Ma]	Datum Present [mbsl]	Datum Present [m CSF- A]	TWT (seconds)
II	Base <i>Globorotalia truncatulinoides</i>	PF	1.93	316.2	51.9	0.409
	Top <i>Globigerinoides extremus</i>	PF	1.99	325.1	60.84	0.419
	Horizon H7					0.451
	Base <i>Globorotalia tosaensis</i>	PF	3.35	390.6	126.30	0.494
	Top <i>Dentoglobigerina altispira</i> (Pacific)	PF	3.47	391.7	127.4	0.495
III	Top <i>Globorotalia margaritae</i>	PF	3.85	427.3	163.00	0.535
	<i>Pulleniatina</i> coiling sinistral to dextral	PF	4.08	454.0	189.65	0.564
	Top <i>Sphaeroidinellopsis kochi</i>	PF	4.53	492.7	228.35	0.606
	Horizon H6					0.657
IV	Top <i>Discoaster quinqueramus</i>	CN	5.59	545.7	281.39	0.662
	Top <i>Reticulofenestra rotaria</i>	CN	6.25	577.1	312.75	0.695
	Horizon H5					0.768
V	Top <i>Flosculinella</i> above Base	LBF	11.6	717.8	453.5	0.794
	<i>Calcidiscus macintyreii</i>	CN	13.36	844.2	579.91	0.876
	Horizon H4					0.916
V	Horizon H3					0.962
	Base <i>Nephrolepidina ferreroi</i>	LBF	16	1009.3	745	0.997

first interpret the morphology of the drowned reef at the Rowley Shoals (Fig. 3A). It was also the profile used during IODP Expedition 356 to select IODP Site U1464 (Gallagher et al., 2017b). Expedition SO257 (Kuhnt et al., 2018) repeated this line as part of its ship track, acquiring high-resolution seismic (Fig. 3B) and sub-bottom profile data (Fig. 3C) over the same area.

The high-resolution seismic data across IODP Site U1464 shows a good correlation between lithology and seismic facies (Figs. 2, 4). The series of parallel low-medium amplitude reflectors from ~0.36 to 0.40 s, and from 0.51 to 0.66 s TWT correlate to the mud facies of Units I and III. The chaotic and disrupted sub-parallel reflectors from 0.40 to 0.45 s correlate to the upper part of Unit II. The lower amplitude reflectors directly underlying this section from 0.45 to 0.51 s correlate to the lower half of Unit II and an increase in siliciclastics in this unit. The parallel low-medium amplitude reflectors of Unit III onlap onto the underlying H6 horizon (Base Pliocene; at ~0.66 s). Below the latest Miocene-Pliocene H6 Horizon low-medium amplitude chaotic and disrupted sub-parallel reflectors are present until the Late Miocene H5 Horizon (0.77 s), where the reflectors become sub-parallel with high amplitudes to ~0.84 s, near the base of Unit IV. Below 0.84 s at Site U1464 (Fig. 4) reflectors have lower amplitudes with complex mix of parallel, sub-parallel, chaotic and disrupted reflectors to the base of the section cored at Site U1464 at ~1.06 s.

Many of the reflectors at IODP Site U1464 can be mapped laterally to the leeward side of the drowned Rowley Shoal (Figs. 4, 5, 6). Between the latest Miocene-Pliocene H6 Horizon and the base of Unit II, the parallel low-medium amplitude reflectors show an aggradational reef growth phase. Reflector geometry shifts from aggradational to back-stepping above the base of Unit II until the Late Pliocene-Pleistocene H7 Horizon. Reef growth at this location terminates at the H7 Horizon (~0.45 s) with reflectors onlapping the leeward side of the reef to the

seafloor. On the windward side (Fig. 6), a moat around the base of the drowned reef and associated sediment drift features are present in seismic and sub-bottom profile data (Figs. 6, 7). An interval of disrupted reflectors is present beneath the Late Pliocene-Pleistocene H7 Horizon (Fig. 6). This feature is associated with reef talus shed from the margin of the reef. Similar to the leeward side of the reef, this area shows strong onlap of reflectors onto the H7 Horizon. Sub-bottom profile data shows a central lagoon, with similar geometry to the modern Rowley Shoals (Figs. 1, 7).

7. Reconstructing the geometry of the drowned Rowley Shoal

In this study, 146 2D seismic profiles obtained from 10 seismic surveys were analysed within the drowned reef work area (Area B; Figs. 1, 8). Mapping of the major drowning horizon (H7) revealed that the final stage of the drowned reef exhibited multiple components that made up the reef system (Fig. 8).

The main north-south oriented drowned atoll (Fig. 8) is similar in morphology to the modern Rowley Shoals. It is 17 km long and 10 km wide with a central lagoon, and a steeper windward reef front compared to the leeward side (Figs. 8, 9).

There is a secondary atoll present to the south of the main atoll (Fig. 8) with a different morphology to the modern Rowley Shoals (Figs. 8, 10). In 2D seismic profiles, this reef is not as well defined as the main atoll. It is characterised by intervals of disrupted reflectors with highly variable amplitudes and occasional atoll-like features such as a steep windward margin (Fig. 10 I) with a possible central lagoon (Fig. 10 L).

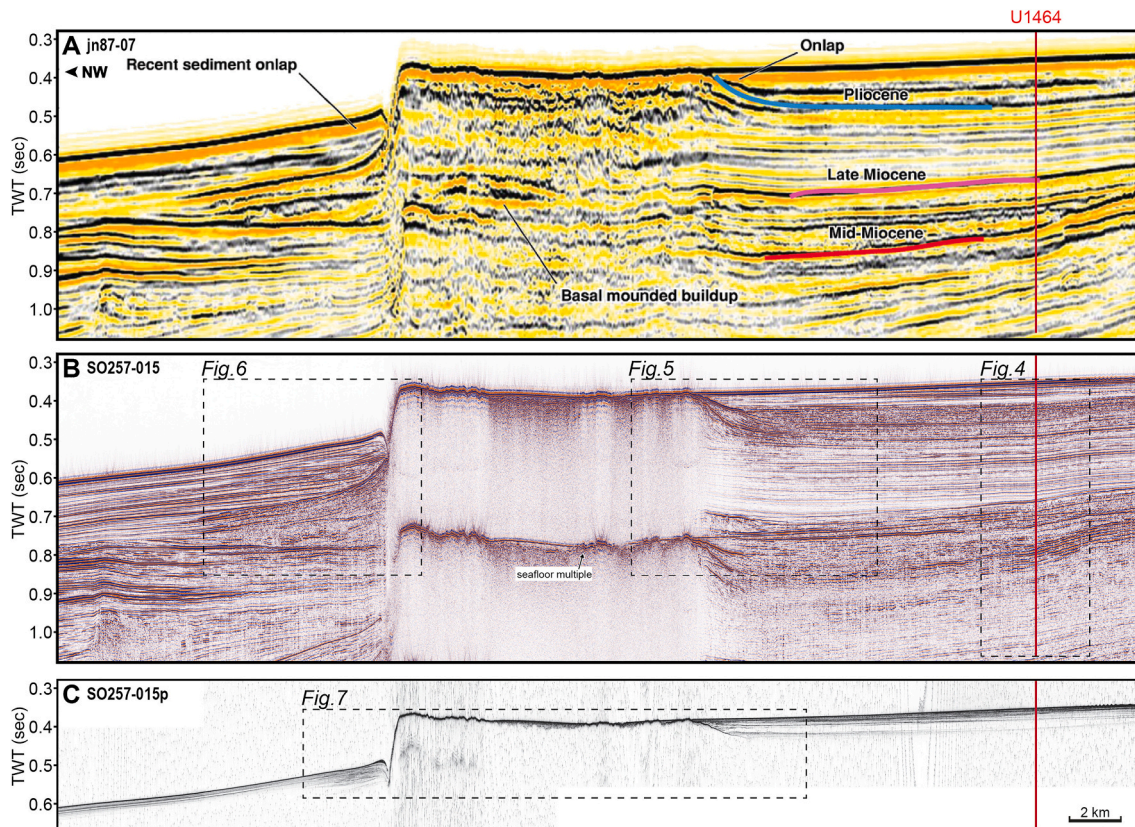


Fig. 3. Seismic lines across the drowned Rowley Shoal A) Interpreted industry 2D seismic profile (line jn87-07 adapted from Ryan et al., 2009 with their interpreted ages for reflectors) showing the location of IODP Site U1464. B) A high-resolution 2D seismic profile (SO257-015) across line jn87-07 acquired by the RV *Sonne* Expedition 257 (Kuhnt et al., 2018). C) Matching sub-bottom profile (SO257-015p) from RV *Sonne* Expedition 257 (Kuhnt et al., 2018). Line locations are on Fig. 1.

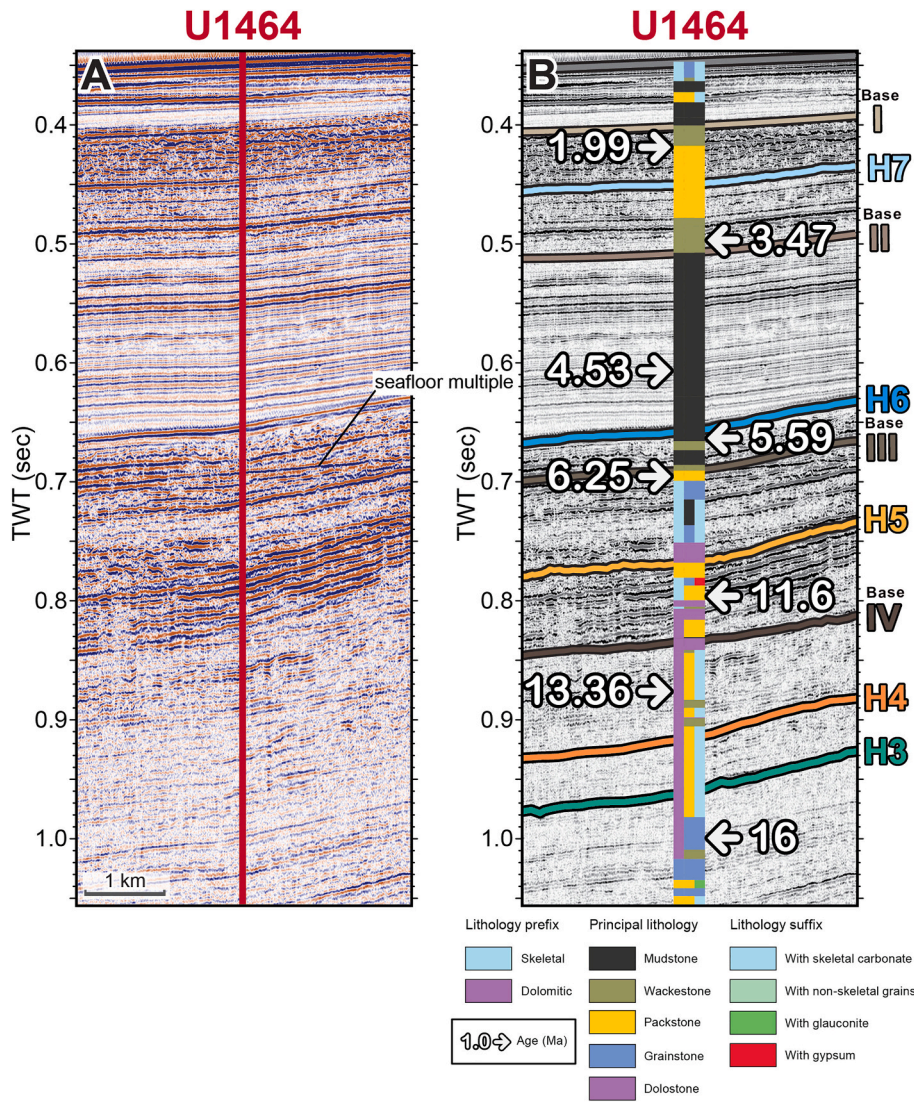


Fig. 4. A) Uninterpreted section of 2D seismic profile SO257-015 (see Fig. 3 for location) at Site U1464. B) Composite lithology log and ages for IODP Site U1464 overlain on interpreted seismic horizons (H3 to H7) and the base of Units I to IV.

8. The Miocene to recent development of the drowned “fourth” Rowley Shoals

The detailed seismic analyses described above reveals the following history of the drowned fourth Rowley Shoals. An initial Middle Miocene barrier reef platform developed (MioR-1 and MioR-2; Figs. 9 G, 11). This was followed major backstepping and Late Miocene isolated atoll growth (MioR-3 IA; Figs. 9 G, 11) and reef growth termination at the latest Miocene to Pliocene H6 Horizon (Fig. 11). Reef growth was absent above the latest Miocene to Pliocene H6 Horizon in the southern part of the drowned shoal (Fig. 10), while the presence of buildups in the central (Fig. 9 E, F and G) and northern sections and presence of reef talus above the H6 horizon suggests continued reef growth into the latest Miocene and Pliocene (Fig. 9 A and B). Major reef expansion initiated on the windward (seaward) side of the drowned shoal occurred during the Pliocene (PlioR-1; Figs. 9 E, F and G, 10H and 11). Reef growth expanded south and on the leeward side of this shoal during the Pliocene (landward; PlioR-2; Figs. 9, 10 and 11) followed by reef growth termination at the Late Pliocene to Pleistocene H7 Horizon.

9. Miocene foundations of the Rowley Shoals

The stratigraphy of the Rowley Shoals area was interpreted using 356 2D seismic profiles from 13 seismic surveys (Study Area A; Fig. 1). Mapping of the top of the barrier reef facies (top MioR-2, McCaffrey et al., 2020) suggests that the locations of the drowned reef and modern Rowley Shoals were controlled by the antecedent Miocene barrier reef geometry (Figs. 12, 13).

The Miocene barrier reef reached its maximum extent between the H4 and H5 Horizons during the Middle Miocene (MioR-2 SRM; seaward-most reef margin; Fig. 14). Subsequently, reef growth backsteps above the Late Miocene H5 Horizon, transitioning to several isolated atolls and pinnacle reefs (MioR-3 in Figs. 13, 14). These Late Miocene isolated atolls/pinnacles underlie and are present between the Rowley Shoals (Fig. 14), and to the north of the study area (Fig. 1). However, reefs are absent south of the drowned shoal. The majority of Late Miocene MioR-3 reefs cease their growth at the H6 horizon (Figs. 13, 14).

The continuance of Pliocene reef aggradation above the H6 Horizon is shown by the presence reef talus in seismic profiles associated with the drowned reef (Figs. 9, 13), Imperieuse Reef (Figs. 13, 14), Clerke Reef (Fig. 14), and Mermaid Reef (Fig. 14). This seismic facies terminates or contracts at the Late Pliocene-Pleistocene H7 horizon and re-occurs only

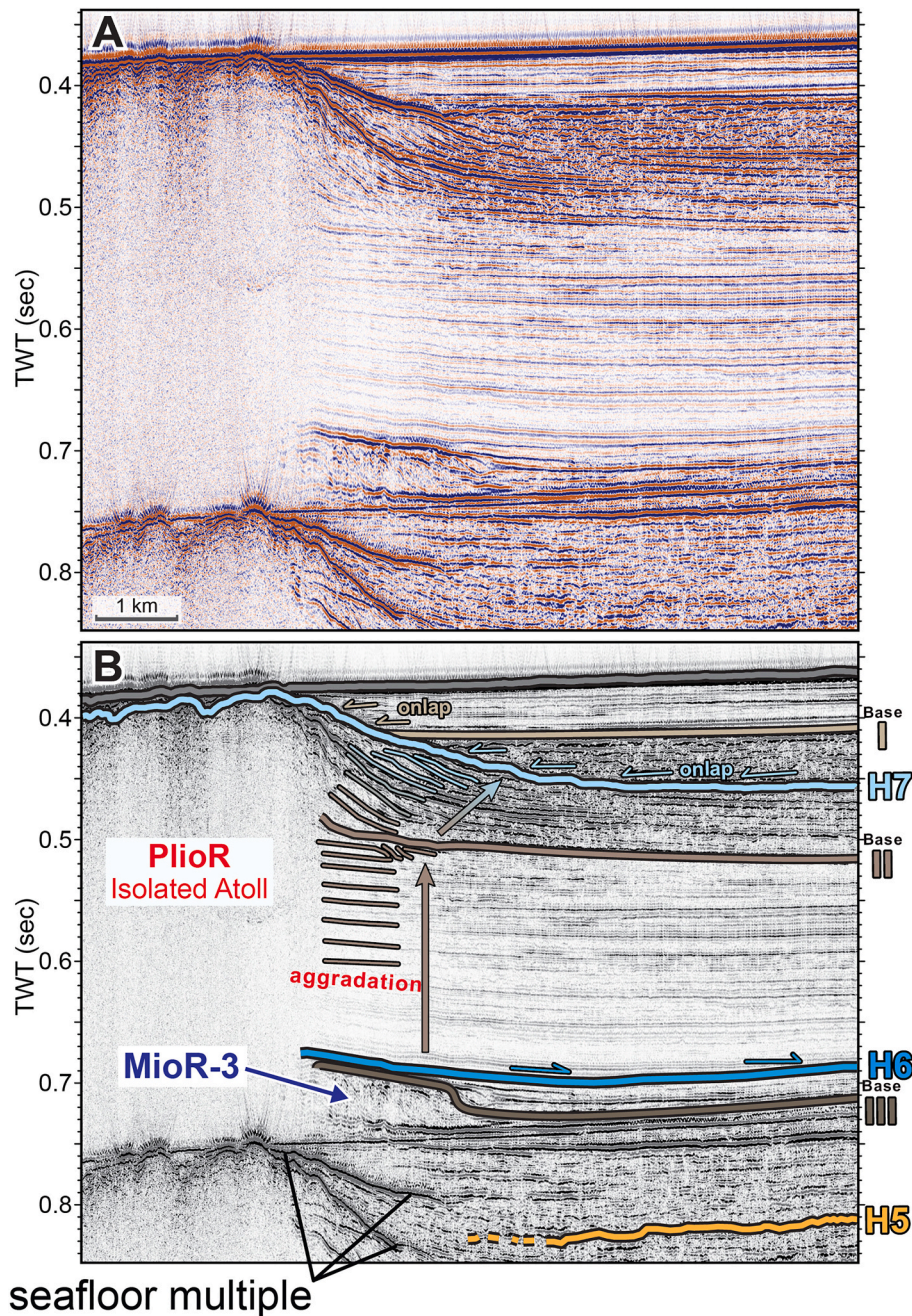


Fig. 5. A) Uninterpreted section of 2D seismic profile SO257–015 (see Fig. 3 for location) over the south-eastern (leeward/landward) edge of the drowned shoal. B) Interpreted seismic horizons and lithology boundaries from Site U1464, showing their interaction with the drowned shoal and an underlying Miocene patch reef (MioR-3). Unconformable contact onto each of the latest Miocene-Pliocene H6 and Late Pliocene-Pleistocene H7 horizons is indicated by the onlap of the overlying strata. The strata between the H6 and H7 have an aggradational geometry to the base of Unit II, followed by backstepping (or aggradation of the platform generating an increased depositional dip) to the H7 horizon.

in the modern three Rowley Shoals (Fig. 13).

The present Rowley Shoals are 10 km seaward of a major fault zone (Mermaid Fault Zone; Figs. 1, 14). This fault zone is not present in 2D seismic profiles south of Imperieuse Reef (Figs. 11, 14). The Late Miocene H6 Horizon drowning and burial event further restricts reef growth to north of 18°S leaving three modern Rowley Shoals, with the southerly drowned shoal drowning by the Late Pliocene-Pleistocene H7 Horizon (~ 3 Ma).

10. Discussion

The Rowley Shoals are built upon the foundations of a Middle to Late

Miocene “great barrier reef” (McCaffrey et al., 2020, Figs. 1, 15). The oldest reefs in the area, however, are Oligocene in age (34–27.8 Ma; Belde et al., 2017) forming narrow and discontinuous mounded buildups (PalR reefs; Figs. 14). Often directly overlying these buildups, the first Miocene reefs (~17 Ma; MioR-0 reefs) are isolated small, mound-shaped features similar in geometry to the underlying Oligocene reefs (Figs. 14). At around 16 Ma prograding barrier reefs (MioR-1 reefs, Fig. 15) first appears in the Rowley Shoals area, shortly after the onset of the Middle Miocene Climate Optimum (Fig. 16). These have a different geometry and platform shape compared to the underlying reefs, in that they create a relatively continuous series of platforms with distinct reef margin, marginal slope, and back reef facies on seismic profiles (Figs. 11, 14). It

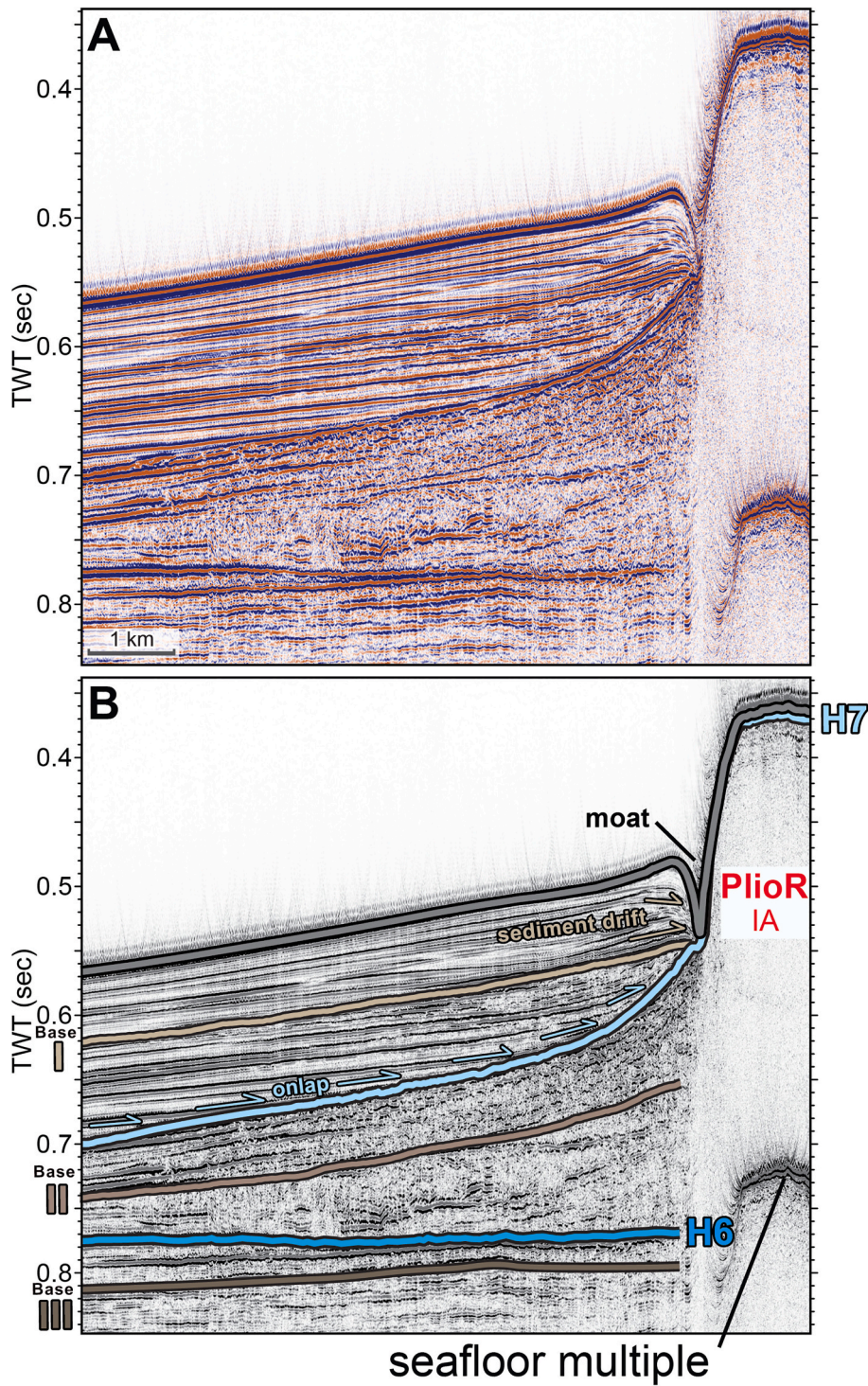


Fig. 6. A) Uninterpreted section of 2D seismic profile SO257-015 (see Fig. 3 for location) over the north-western (windward/seaward) edge of the drowned shoal. B) Interpreted seismic horizons and lithology boundaries from Site U1464, showing their relationship to the drowned shoal. Unconformable contact onto the Late Pliocene-Pleistocene H7 Horizon is indicated by onlap of the overlying strata. Strata above the base of Unit I horizon appear to have interacted with the base of the drowned reef to form a current scour moat and associated sediment drift.

is well known that the Middle Miocene Climate Optimum led to a poleward extension of the global reef belt (Perrin and Kiessling, 2012) and also coincides with the maximum extend of reef growth on the North West Shelf. It therefore seems likely that the warm climate conditions during the Middle Miocene Climate Optimum allowed the formerly isolated reefs to prograde and coalesce into a barrier reef system. The position of Late Miocene atoll and pinnacle reef growth (MioR-

3 reefs) after the major backstepping events around 10 Ma (Fig. 15) is related to the geometry of the underlying progradational reefs (MioR-1,2 reefs), with the atoll/pinnacle growth backstepping to a position where the underlying reef system is thickest (Fig. 14). This is probably a function of compaction, where the muddy lithologies around the limestone reefs compact more than the reefs themselves, leading to less subsidence where the reefs are thickest (Hunt and Fitchen, 1999;

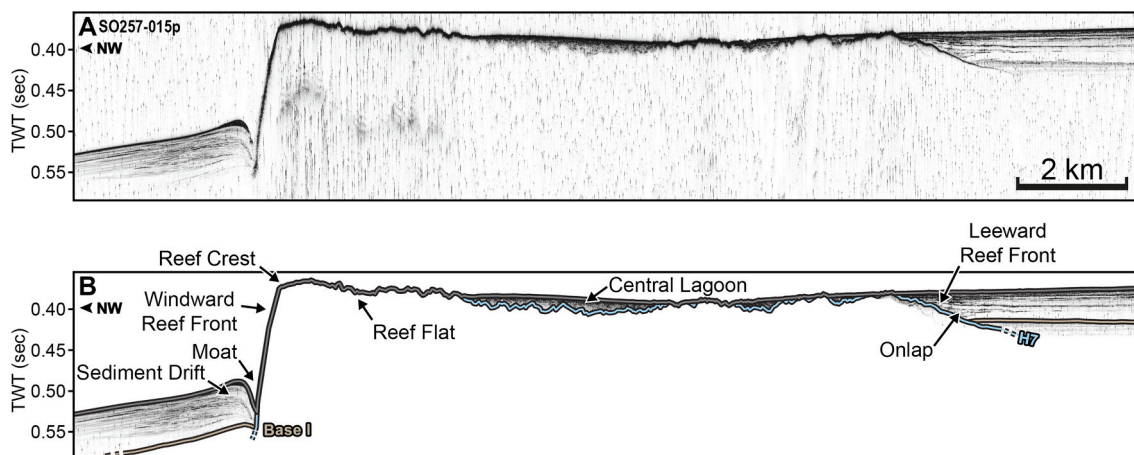


Fig. 7. A) Uninterpreted section of sub-bottom profile SO257–015p (see Fig. 3 for location) over the drowned reef. B) Interpreted seismic horizons and lithology boundaries from Site U1464. Recent sediment is observed infilling the central lagoon of the drowned reef. Strata above the base of Unit I on the windward side of the reef appear to have interacted with the base of the drowned reef to form a current scour moat and associated sediment drift. The strata on the leeward side onlaps the H7 horizon.

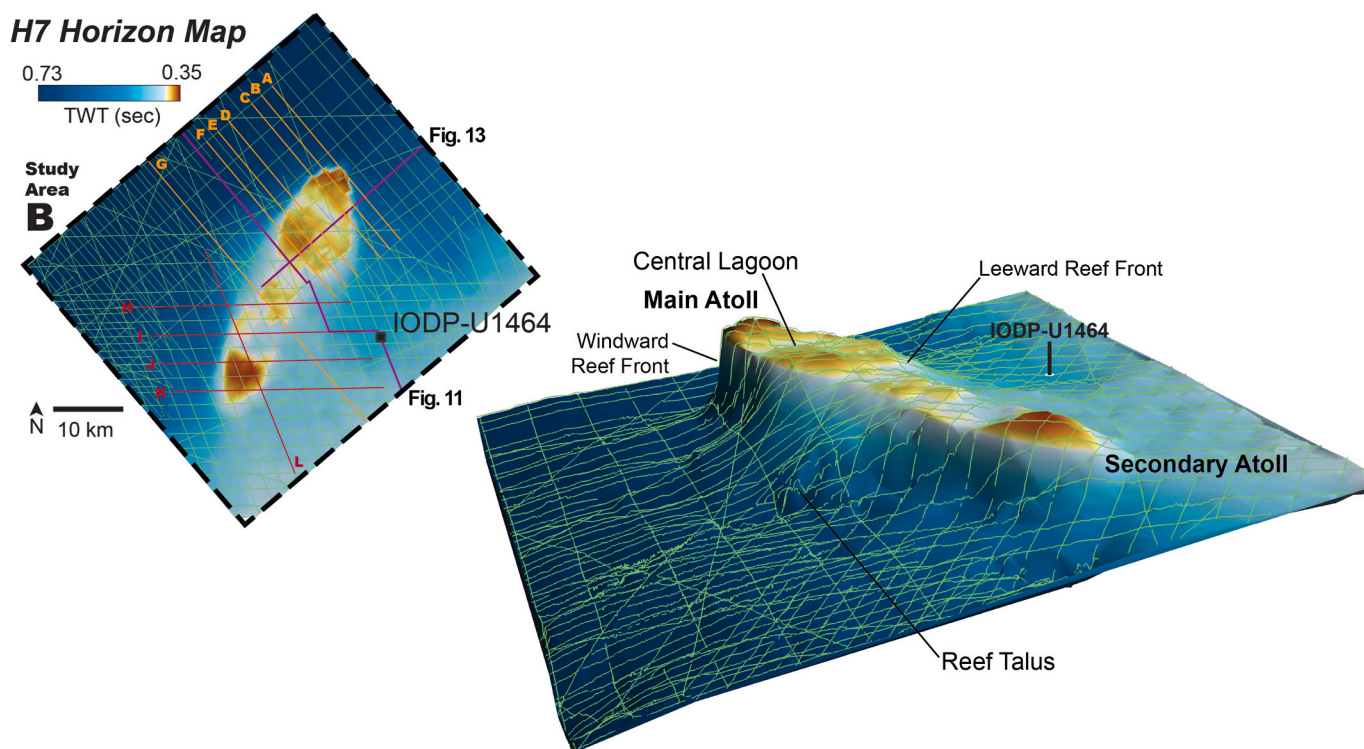


Fig. 8. H7 Horizon TWT structure map of Area B (see Fig. 1 for location). Location of 2D seismic profiles in Fig. 9 are orange and 2D seismic profiles in Fig. 10 are red. Right) 3D view of TWT structure map and interpretation of the drowned Rowley Shoals facies of the H7 Horizon. (For interpretation of the references to colour in this figure legend, the reader is referred to the web version of this article.)

McCaffrey et al., 2020). The position of these Late Miocene reefs then determines the position of the drowned Pliocene reef and the Rowley Shoals that survive into present.

10.1. Horizon H6: Miocene-Pliocene reef extinction

A major reef extinction event occurs across the Miocene-Pliocene boundary on the North West Shelf (Rosleff-Soerensen et al., 2012; McCaffrey et al., 2020; Groeneveld et al., 2017; Steinhorsdottir et al., 2021). This reef extinction event terminates Late Miocene reef growth (MioR-3) locally and coincides approximately with the regional base

Pliocene seismic reflector horizon (SB5, Rosleff-Soerensen et al., 2016; BB5, Van Tuyl et al., 2018a; H6 Horizon, this work, Fig. 15). Locally around the Rowley Shoals, the H6 Horizon (~ 5.6 Ma) coincides with a major change in seismic facies. In the southern portion of the drowned Rowley Shoal, this reflector can be mapped continuously under the reef (Figs. 9, 10), suggesting that reef growth ceased by H6 time. In the nearby IODP Site U1464, Gallagher et al. (2017b) documented a change in lithology just below the H6 Horizon (their Unit III/IV boundary). The Unit III/IV boundary represents a change from carbonate-rich to relatively carbonate-poor lithologies.

The stratigraphic events across the Miocene-Pliocene boundary are,

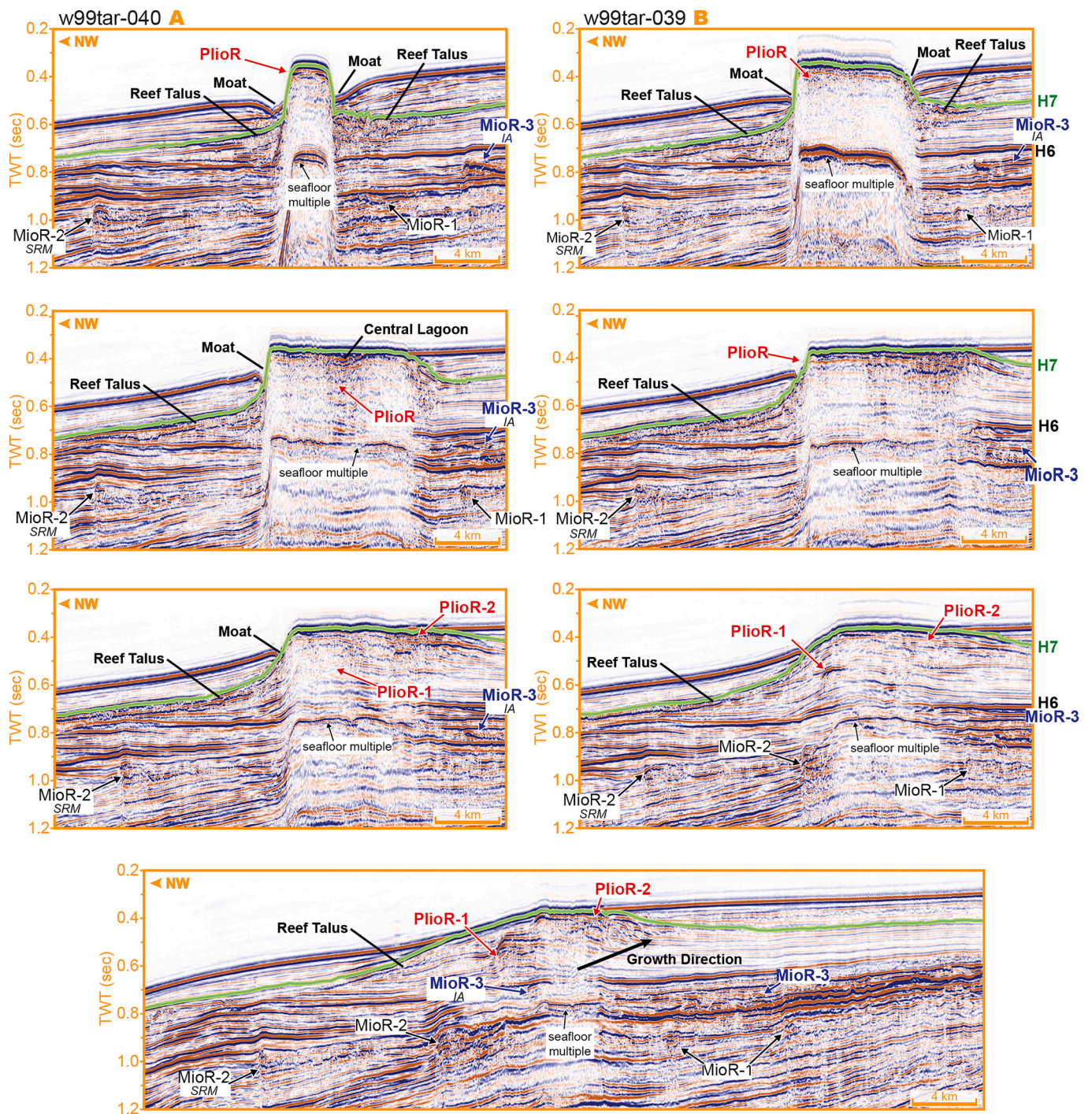


Fig. 9. 2D seismic profiles over the northern/central portion of the drowned Rowley Shoal used create the H7 horizon TWT structure map (green line) in Fig. 8. (For interpretation of the references to colour in this figure legend, the reader is referred to the web version of this article.)

as a first approximation, most readily interpreted as a significant transgression. This is consistent with the paleo-water-depth estimates by Gallagher et al. (2017b) and Gurnis et al. (2020) who documented a major transgression at around 6 Ma at IODP Sites U1462, U1463 and U1464. While this transgression has a different character and slightly different timing in each of the IODP Sites, it is present in all locations. The estimated magnitude (>200 m deepening) of this transgression led Gurnis et al. (2020) to suggest a tectonic subsidence origin for this deepening.

Based on natural gamma logs from IODP Site U1463, Christensen et al. (2017) suggested a climatic origin for increased siliciclastic input

at ~6 Ma and proposing that it represented the onset of a latest Miocene-Early Pliocene “Humid Interval”. However, subsequent work by Karatsolis et al. (2020) shows that the change to more siliciclastic deposition influx (recorded by gamma logs) is diachronous across the North West Shelf. They suggest that the onset of siliciclastic deposition at a specific site depends on its location relative to the evolving deltaic system and the available accommodation space, both controlled by tectonic subsidence. Karatsolis et al. (2020) therefore suggest that the siliciclastic deposition may have initiated prior to 6 Ma.

Therefore, the H6 Horizon reef extinction event appears to be closely tied to a major episode of tectonic subsidence on the North West Shelf

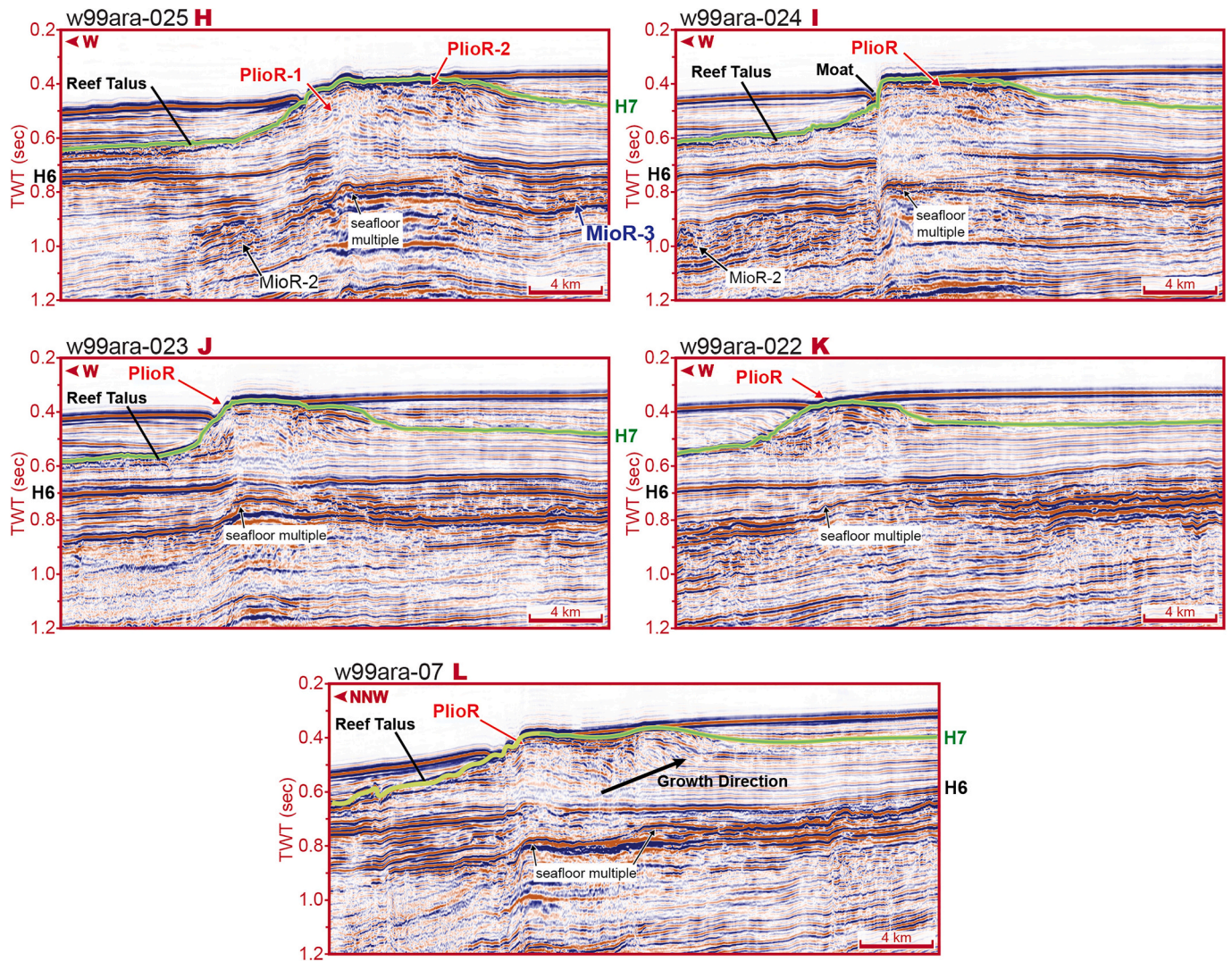


Fig. 10. A selection of 2D seismic profiles over the central/southern portion of the drowned Rowley Shoal used to create the H7 horizon TWT structure map (green line) in Fig. 8.

(Gurnis et al., 2020). For a long time, reef drowning on passive margins was regarded as a paradox, as the growth potential of healthy reefs normally exceeds typical passive-margin subsidence rates (Schlager, 1981). However, it has been shown that negative feedbacks can lead to drowning of healthy reef platforms even if the rate of sea level rise does not exceed the maximum growth potential of the carbonate platform (Kim et al., 2012). Subsidence and drowning are therefore a likely cause for reef cessation. This is also consistent with the position of the younger atoll reefs being above the thickest portions of the barrier reef (i.e. where compaction and hence subsidence is minimized).

It is noteworthy that the Late Miocene to Pliocene reef collapse is not unique to the North West Shelf of Australia. Harrison et al. (2023) postulated a general Pliocene reef gap across the modern Coral Triangle in the central Indo-Pacific. They argued that the decline in reef abundance was controlled by regional tectonic changes such as uplift and subsidence rather than larger-scale controlling factors like climate. In contrast, Petrick et al. (2024b) show that the Late Miocene Cooling between 7 and 5.4 Ma (Fig. 16) led to a rapid temperature drop of $\sim 2^\circ\text{C}$ offshore NE Australia. These authors postulate that this temperature drop and associated changes in the position of rain belts and ocean currents provide a better explanation for the coeval coral reef decline in the entire central Indo-Pacific. This temperature change, along with other stressors linked to the cooling, may also have diminished the

aggradation potential of the North West Shelf reef system. This could have limited its ability to keep up with the relative sea-level due to the tectonic subsidence pulse around 6 Ma.

10.2. Pliocene reef growth

Above the latest Miocene to Pliocene H6 Horizon, reef growth in the Rowley Shoals region slowly re-established, creating the four Rowley Shoals (Fig. 13). These four reefs grew directly above the late Miocene MioR-3 isolated atolls. Topographic inversion related to reactivation of the Mermaid Fault Zone (Figs. 14) during the Late Miocene to Early Pliocene (Keep et al., 2007; Hengesh and Whitney, 2016). This may have contributed to the restart of the reefs of the four Rowley Shoals, as there is no other evidence of Pliocene coral reef growth to the south (Goktas et al., 2016), or to the north until the platform with the modern day Scott and Seringapatam Reefs (Fig. 1, Van Tuyl et al., 2018a, 2018b; Thronberens et al., 2022; Williams et al., 2023). Nor is there any evidence of Pliocene reef growth in the now drowned middle-shelf reef platforms of the Browse Basin (Thronberens et al., 2022). An increase in sea surface temperatures at ~ 4.6 Ma in the Northern Carnarvon Basin (Ocean Drilling Site 763A, Karas et al., 2011; Karatsolis et al., 2020) may have been an additional driver for Early Pliocene reef growth (PlioR-1; Fig. 11).

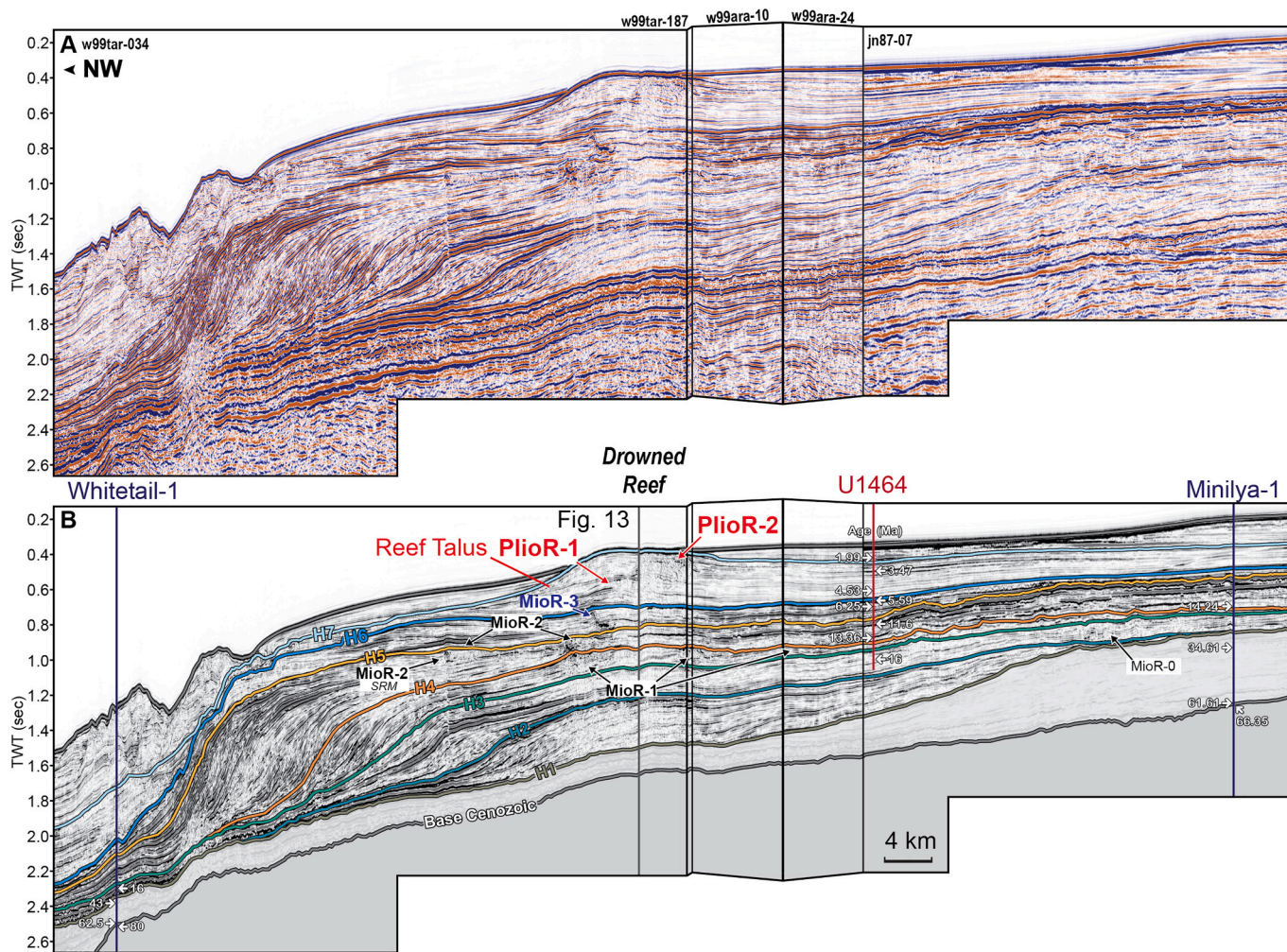


Fig. 11. A) Uninterpreted composite dip seismic profile from the wells Minilya-1 to Whitetail-1, through the central part of the drowned Rowley Shoal (see Fig. 1 for location). B) Interpreted section showing mapped seismic horizons and their relationship to ages from IODP Site U1464, Minilya-1 and Whitetail-1. The earliest reef growth stage is the MioR-0 carbonate buildups, these transition into the barrier reef facies of MioR-1 and MioR-2. The maximum extent of reef growth (MioR-2 SRM; seaward-most reef margin) is followed by backstepping (MioR-3). Pliocene atoll/pinnacle growth (PlioR-1 and PlioR-2) initiated above the H6 Horizon and terminated by the late Pliocene-Pleistocene H7 Horizon.

The second Pliocene growth phase (PlioR-2; from 4 Ma to 2.5 Ma; Fig. 11) coincides with global Late Pliocene warming (Middle Pliocene Warm Period; ~3.3–3 Ma; Salzmann et al., 2011, Westerhold et al., 2020, Fig. 16) and the onset of the modern West Pacific Warm Pool (Gallagher et al., 2009, 2024). However, while temperatures were warmer in the southwest Pacific at this time, eastern Indian Ocean sea surface temperatures cooled by around 4 °C (from 3.5 to 3 Ma; Karas et al., 2009; De Vleeschouwer et al., 2018). This cooling is interpreted to be related to Indonesian seaway constriction and a reduction in intensity of the southward flowing Leeuwin Current (Cane and Molnar, 2001; Karas et al., 2011; Auer et al., 2019; Gallagher et al., 2024). Despite this cooling, the four Rowley Shoals continued to grow through this period, while inner to middle shelf reefs towards the north in the Browse Basin drowned during this time (Thronberens et al., 2022).

Global sea level fluctuations throughout the Early Pleistocene (Miller et al., 2020; Rohling et al., 2021, Fig. 16) may also have influenced the morphology of the drowned shoal. Since the beginning of the Pleistocene at about 2.6 Ma, ice volume increases through time have resulted in increased sea level amplitude (Miller et al., 2020; Rohling et al., 2021, Fig. 16). This may have temporarily exposed the drowned shoal and karstified its upper surface. Maximum dissolution in the centre of the exposed platform may have created the depression across the drowned shoal (Fig. 7), which is surrounded by the raised rims where the rates of

dissolution would be minimum (cf. Droxler and Jorry, 2021). Alternatively, the lagoonal interior of the atoll may simply be caused by high rates of relative sea-level rise, as first suggested by Charles Darwin (Darwin, 1842) and consistent with high tectonic subsidence rates in the region during this period (Czarnota et al., 2013; Gurnis et al., 2020).

10.3. H7 Horizon: Pleistocene reef drowning

By the Early Pleistocene (Gelasian) the southernmost reef in the Rowley Shoals region (H7 Horizon) drowned while the other three northerly shoals persisted to present. IODP Site U1464 shipboard age data suggest a 2.4 Ma age (Gallagher et al., 2017b) for the H7 Horizon (0.45 s TWT; ~88 m CSF-A, Fig. 2). A revised age model for Site U1463 (Groeneveld et al., 2021), when correlated to U1464, suggests that the H7 horizon (~88 m WMSF) may be as young as ~1.9 Ma. Thus, the fourth Rowley Shoal drowned between 1.9 and 2.4 Ma in the Early Pleistocene.

This event may be related to reorganization of Indian Ocean circulation after ~2.4 Ma, and the transition from humid to arid conditions (Christensen et al., 2017). Counter to the evidence of reef termination, more arid conditions and the associated reduction in terrestrial siliclastic input might be expected to improve conditions for reef growth. However, Indonesian Throughflow constriction and the reduction in

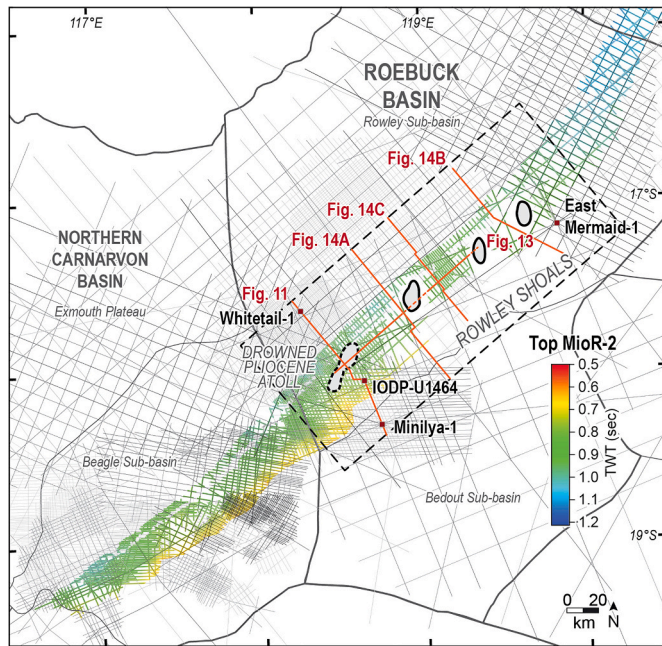


Fig. 12. Top MioR-2 the last stage of barrier reef growth adapted from McCaffrey et al. (2020) and TWT structure map of the Rowley Shoals (dashed line rectangle). Position of the modern Rowley Shoals (black line with grey infill) and the drowned (black dashed line with grey infill) are approximately 10 km from the seaward-most reef margin of MioR-2. Location of 2D seismic profiles are in grey. (For interpretation of the references to color in this figure legend, the reader is referred to the web version of this article.)

intensity of the Leeuwin Current after 2.4 Ma (Gallagher et al., 2009, 2014) may have led to a cooling and an increase in regional upwelling in the Rowley Shoals area (see also Smith et al., 2020). This cooling and upwelling together with high amplitude glacio-eustatic sea level variability may have been sufficient to cause local extinction of the most southerly Rowley shoal while the other three Rowley shoals managed to survive until present.

11. Conclusions

The modern Rowley Shoals are a series of three isolated atolls off the northwest coast of Australia. Each ring-shaped atoll rises from 250 m depths representing the remnants of an ancient 2000 km long great barrier reef that stretched from the Timor Sea in the northeast to Cape Range in southwest during the Miocene. Marine seabed and industry seismic surveys reveals a fourth “drowned” Rowley Shoal to the southwest that drowned in the Neogene. Detailed analyses of high resolution and industry seismic surveys, together with coring data near the Rowley Shoals reveal a complex history of expansion and contraction related to subsidence, sea level and climate variability that ultimately caused the demise of one out the four Neogene Rowley Shoals on the tropical North West Australian Shelf.

The first Miocene reefs (~17 Ma) in the Rowley Shoals region were isolated small, mound-shaped features. Prograding barrier reefs first appear during the Middle Miocene at ~16 Ma forming a continuous series of platforms with reef margin, marginal slope, and back reef facies. By around 10 Ma, atoll/pinnacle reefs backstepped landward to a position where the underlying barrier reef system was the thickest. A major reef drowning event occurs across the Miocene-Pliocene boundary terminated Late Miocene reef growth. This coincides with a major change in from carbonate-rich to relatively carbonate-poor facies due to

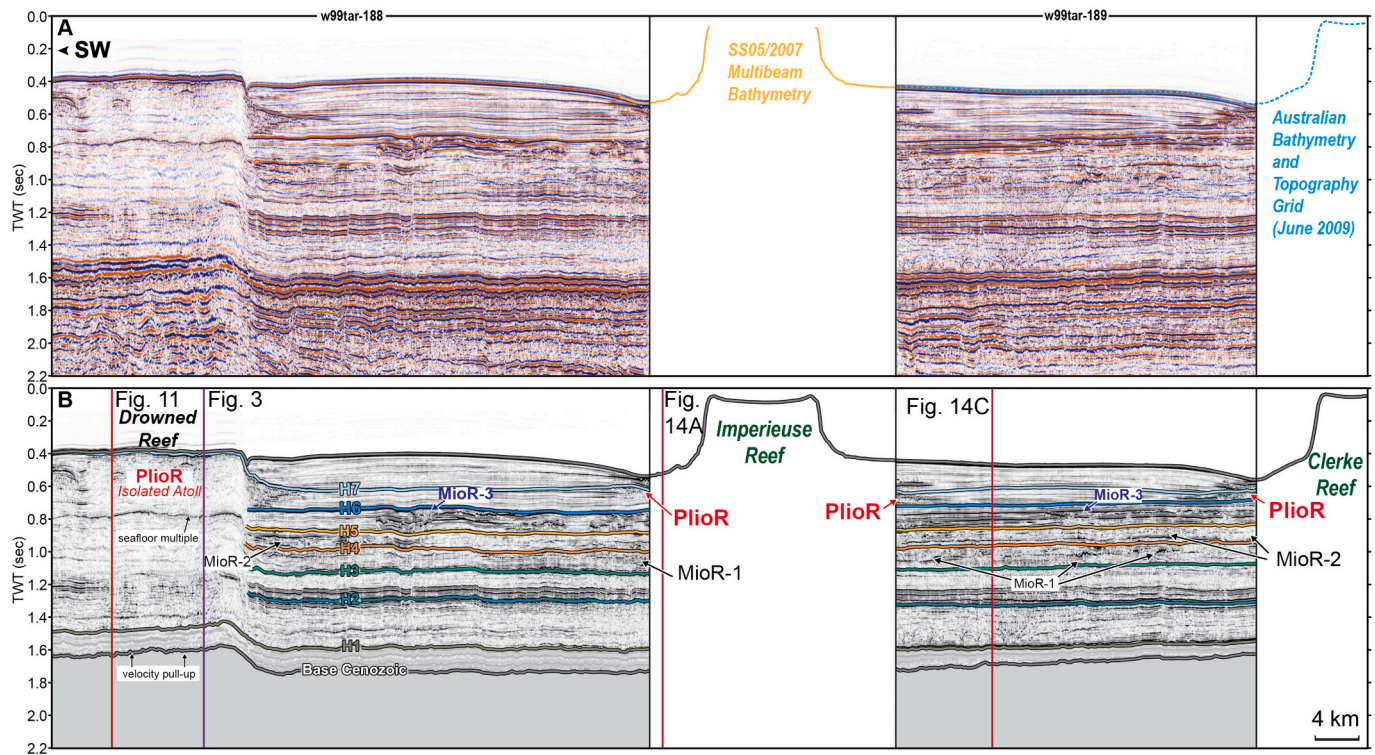


Fig. 13. A) Composite strike seismic profile through the drowned Rowley Shoal, Imperieuse Reef and Clerke Reef (see Figs. 1, 12 for location). Southern Surveyor Voyage SS05/2007 high resolution multibeam bathymetry is used to map Imperieuse Reef (yellow line). Data is converted from metres (below sea level) to TWT (seconds) using the measured sonic velocity of water above the seafloor (V_w ; m/s) in the Minilya-1 well. Australian Topographic and Bathymetric Grid (2009) multibeam data across Clerke Reef are converted to TWT (sec). B) Interpreted section showing mapped seismic horizons and reef growth stages. The reef talus facies associated with the drowned reef is also present in the modern Clerke and Imperieuse Reefs. (For interpretation of the references to colour in this figure legend, the reader is referred to the web version of this article.)

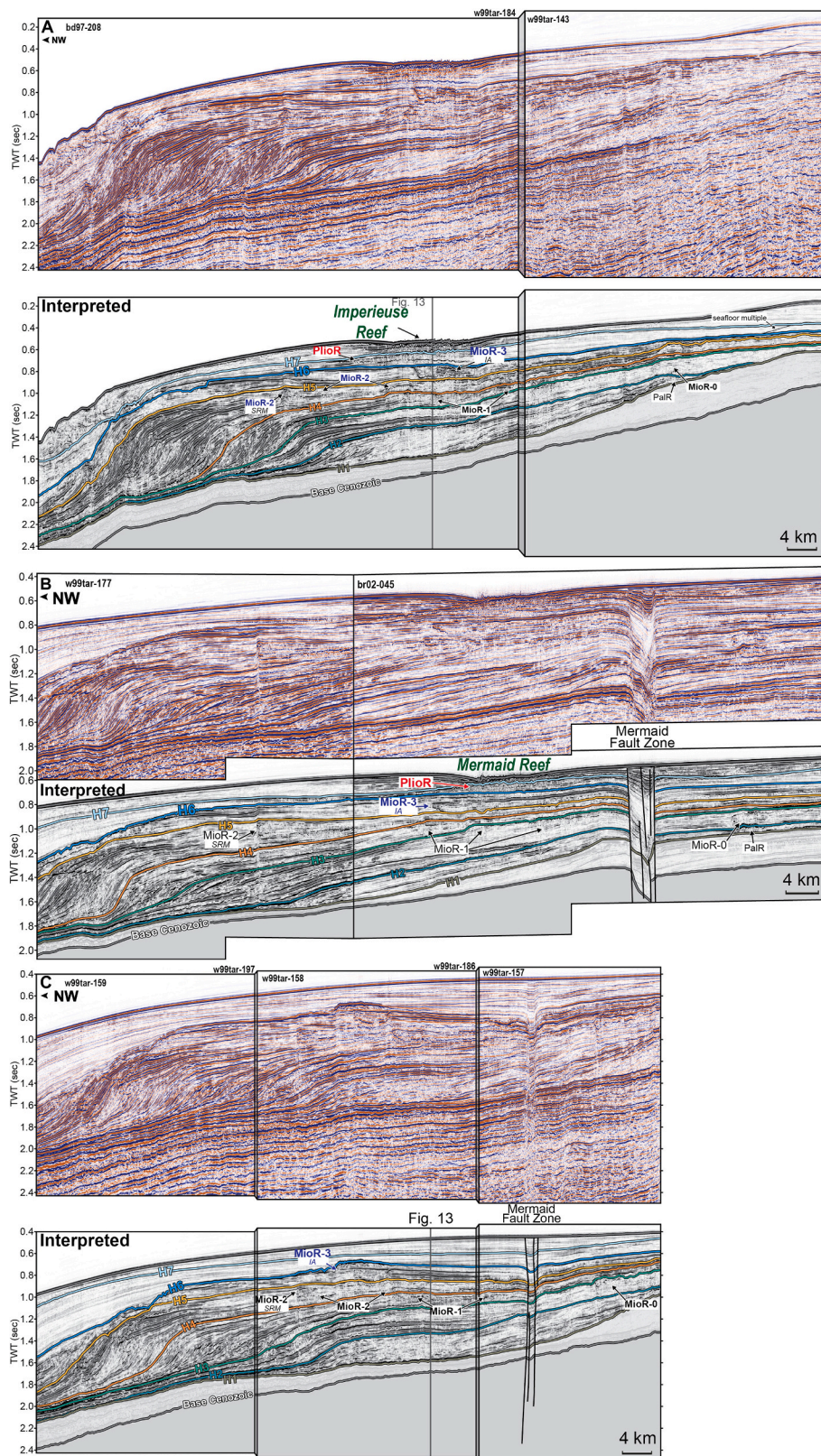


Fig. 14. Composite dip seismic profiles south of A) Imperieuse Reef; B) Mermaid Reef and C) the region between Clerke and Imperieuse Reefs (see Fig. 12 for location). The interpreted sections show mapped seismic horizons and reef growth stages. Earliest reef growth stages are the PalR and MioR-0 carbonate buildups, transitioning to barrier reef facies of MioR-1 and MioR-2. This is followed by backstepping and isolated atoll/pinnacle growth (MioR-3 IA). Pliocene (PlioR) to recent talus facies are associated with the Imperieuse and Mermaid Reefs.

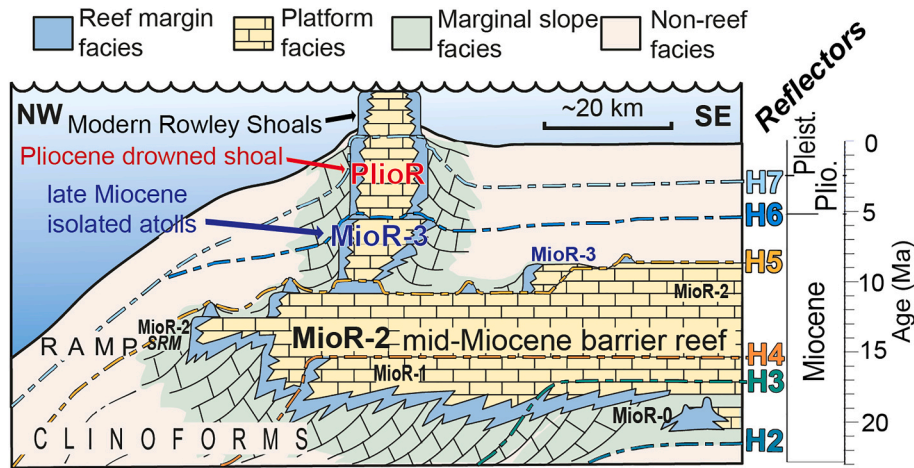


Fig. 15. Neogene reef development of the Rowley Shoals (adapted from McCaffrey et al., 2020) Subsidence and aggradation since the Middle Miocene resulted in limiting reef growth to a series of Late Miocene isolated atolls (MioR-3) forming the foundations for four Rowley Shoals (PlioR). The relationship between reef growth phases and global environmental events is in Fig. 16.

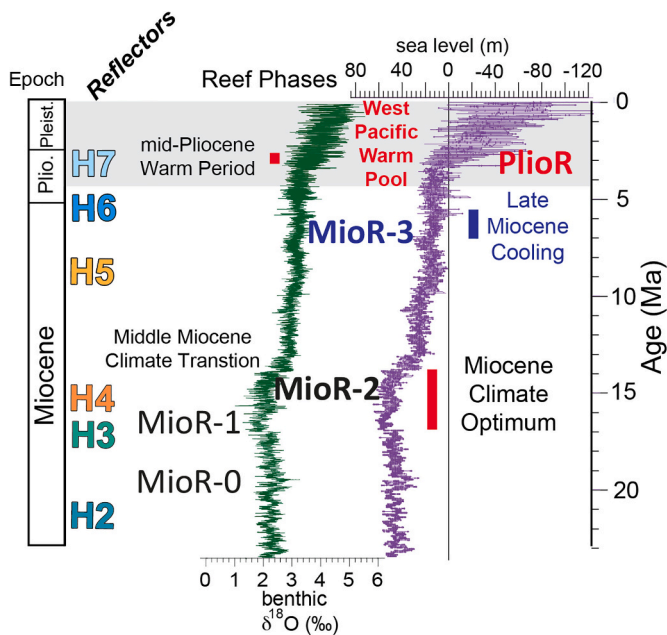


Fig. 16. The relationship between North West Australian Neogene reef growth phases (Fig. 15) to global climatic events (Westerhold et al., 2020) and sea level (Rohling et al., 2021). Late Miocene Cooling is indicated (Herbert et al., 2016). The shading indicates the Pliocene onset of the modern West Pacific Warm Pool (Gallagher et al., 2009, 2024).

increased sea level and regional tectonic subsidence, potentially in combination with the Late Miocene Cooling.

Reef expansion during the Early Pliocene in the Rowley Shoals region may be related to topographic inversion on the Mermaid Fault Zone, together with Early Pliocene warmth starting at ~4.6 Ma. A second Pliocene reef growth phase from ~3.5 to 3 Ma coincides with a period of global Late Pliocene warming and the onset of the modern West Pacific Warm Pool in the southwest Pacific. Reef growth persisted in the region, when eastern Indian Ocean sea surface temperatures had cooled by around 4 °C related to Indonesian seaway constriction and a reduction in intensity of the southward flowing Leeuwin Current.

By the Early Pleistocene (~2 to 2.4 Ma) the most southerly Rowley Shoal had drowned. Indonesian Throughflow constriction and reduction in intensity of the Leeuwin Current after 2.4 Ma may have led to further

cooling and enhanced regional upwelling. These factors together with the prevalence of high amplitude glacio-eustatic sea level oscillations may have been sufficient to cause local extinction of the most southerly Rowley Shoal while the northerly three Rowley Shoals persisted until the present day.

CRediT authorship contribution statement

Jackson C. McCaffrey: Writing – review & editing, Writing – original draft, Validation, Methodology, Investigation, Formal analysis, Conceptualization. **Stephen J. Gallagher:** Writing – review & editing, Supervision, Resources, Conceptualization. **Malcolm W. Wallace:** Writing – review & editing, Supervision, Resources, Conceptualization. **Tanita Averages:** Methodology, Data curation. **Stanislaus G. Fabian:** Writing – review & editing, Methodology. **Katja Lindhorst:** Methodology, Data curation. **Lars Reuning:** Writing – review & editing, Resources. **Sebastian Krastel:** Resources, Investigation, Formal analysis.

Declaration of competing interest

The authors declare that they have no known competing financial interests or personal relationships that could have appeared to influence the work reported in this paper.

Acknowledgements

An Australian Government Research Training Program Scholarship is supporting J. McCaffrey. We would like to thank IHS Markit for their donation of the Kingdom seismic interpretation software. Funding was provided to S.J.G. by the Australian IODP office.

Data availability

Data will be made available on request.

References

Anell, I., Wallace, M.W., 2020. A fine balance: Accommodation dominated control of contemporaneous cool-carbonate shelf-edge clinoforms and tropical reef-margin trajectories, North Carnarvon Basin, Northwestern Australia. *Sedimentology* 67, 96–117.
 Aporthe, M., 1988. Cainozoic depositional history of the North West Shelf. *Aust. Pet. Explor. Soc. Aust.* 55–84.
 Auer, G., De Vleeschouwer, D., Smith, R.A., Bogus, K., Groeneveld, J., Grunert, P., Castañeda, I.S., Petrick, B., Christensen, B., Fulthorpe, C., Gallagher, S.J., 2019.

- Timing and pacing of Indonesian Throughflow restriction and its connection to late Pliocene climate shifts. *Paleoceanogr. Paleoclimatol.* 34 (4), 635–657.
- Australian Geological Survey Organisation, 2001. Interpretation of Geoscience Australia's regional seismic data, offshore northern and northwestern Australia: Survey 94, 95, 98, 100, 101, 106, 110, 116, 118, 119, 120, 128 and 130—digital horizon and fault data in ASCII format. In: Australian Geological Survey Organisation Catalog No's 35232, 35234, 35237, 35239, 35240, 35241, 35242, 35249, 35243, 35244, 35245, 35247, 35248.
- Belde, J., Back, S., Bourget, J., Reuning, L., 2017. Oligocene and miocene carbonate platform development in the browse basin, Australian Northwest Shelf. *J. Sediment. Res.* 87, 795–816. <https://doi.org/10.2110/jsr.2017.44>.
- Bellwood, D.R., Hughes, T.P., Folke, C., Nyström, M., 2004. Confronting the coral reef crisis. *Nature* 429 (6994), 827–833.
- Berry, P.F., Marsh, L.M., 1986. Faunal Surveys of the Rowley Shoals, Scott Reef and Seringapatam Reef, North-Western Australia. Records of the Western Australian Museum, Supplement, p. 25.
- Burgess, P.M., Winefield, P., Minzoni, M., Elders, C., 2013. Methods for identification of isolated carbonate buildups from seismic reflection data. *AAPG Bull.* 97, 1071–1098. <https://doi.org/10.1306/12051212011>.
- Cane, M.A., Molnar, P., 2001. Closing of the Indonesian seaway as a precursor to east African aridification around 3–4 million years ago. *Nature* 411 (6834), 157–162.
- Cathro, D.L., Karner, G.D., 2006. Cretaceous–Tertiary inversion history of the Dampier Sub-basin, northwest Australia: Insights from quantitative basin modelling. *Mar. Pet. Geol.* 23, 503–526. <https://doi.org/10.1016/j.marpetgeo.2006.02.005>.
- Cathro, D.L., Austin, J.A.J.R., Moss, G.D., 2003. Progradation along a deeply submerged Oligocene–Miocene heterozoan carbonate shelf: how sensitive are clinoforms to sea level variations? *AAPG Bull.* 87, 1547–1574.
- Christensen, B.A., Renema, W., Henderiks, J., De Vleeschouwer, D., Groeneveld, J., Castañeda, I.S., Reuning, L., Bogus, K., Auer, G., Ishiwa, T., McHugh, C.M., Gallagher, S.J., Fulthorpe, C.S., Expedition 356 Scientists, 2017. Indonesian Throughflow drove Australian climate from humid Pliocene to arid Pleistocene. *Geophys. Res. Lett.* 44, 6914–6925. <https://doi.org/10.1002/2017GL072977>.
- Coker, D.J., Wilson, S.K., Pratchett, M.S., 2014. Importance of live coral habitat for reef fishes. *Rev. Fish Biol. Fish.* 24, 89–126.
- Collins, L.B., 2002. Tertiary foundations and Quaternary evolution of coral reef systems of Australia's North West Shelf. In: Keep, M., Moss, S.J. (Eds.), *The Sedimentary Basins of Western Australia 3: Proceedings of Petroleum Exploration Society of Australia Symposium*. Petroleum Exploration Society of Australia, Perth, Western Australia, pp. 129–152.
- Courgeon, S., Bourget, J., Jorry, S.J., 2016. A Pliocene–Quaternary analogue for ancient epeiric carbonate settings: The Malita intrashelf basin (Bonaparte Basin, northwest Australia). *AAPG Bull.* 100 (4), 565–595.
- Czarnota, K., Hoggard, M.J., White, N., Winterbourne, J., 2013. Spatial and temporal patterns of Cenozoic dynamic topography around Australia. *Geochemistry, Geophys. Geosystems* 14, 634–658.
- Darwin, C., 1842. *The Structure and Distribution of Coral Reefs*. Smith, Elder and Co, London.
- De Vleeschouwer, D., Auer, G., Smith, R., Bogus, K.A., Christensen, B.A., Groeneveld, J., Patrick, B., Henderiks, J., Castañeda, I., O'Brien, E., Ellinghausen, M., Renema, W., Reuning, L., Ishiwa, T., McHugh, C.M., Gallagher, S.J., Paliike, H., 2018. The amplifying effect of Indonesian Throughflow heat transfer on late Pliocene southern Hemisphere climate cooling. *Earth Planet. Sci. Lett.* 500, 15–27. <https://doi.org/10.1016/j.epsl.2018.07.0350012-821X>.
- De Vleeschouwer, D., Vahlenkamp, M., Crucifix, M., Pälike, H., 2017. Alternating Southern and Northern Hemisphere climate response to astronomical forcing during the past 35 my. *Geology* 45 (4), 375–378.
- Droxler, A.W., Jorry, S.J., 2021. The origin of modern atolls: Challenging Darwin's deeply ingrained theory. *Annu. Rev. Mar. Sci.* 13, 537–573.
- Edgar, G.J., Stuart-Smith, R.D., Willis, T.J., Kininmonth, S., Baker, S.C., Banks, S., Barrett, N.S., Becerro, M.A., Bernard, A.T., Berkhout, J., Buxton, C.D., 2014. Global conservation outcomes depend on marine protected areas with five key features. *Nature* 506 (7487), 216–220.
- Fairbridge, R.W., 1950. Recent and Pleistocene coral reefs of Australia. *J. Geol.* 58 (4), 330–401.
- Gallagher, S.J., Wallace, M.W., Li, C.L., Kinna, B., Bye, J.T., Akimoto, K., Torii, M., 2009. Neogene history of the West Pacific warm Pool, Kuroshio and Leeuwin currents. *Paleoceanography* 24, PA1206. <https://doi.org/10.1029/2008PA001660>.
- Gallagher, S.J., Wallace, M.W., Hoiles, P.W., Southwood, J.M., 2014. Seismic and stratigraphic evidence for reef expansion and onset of aridity on the Northwest Shelf of Australia during the Pleistocene. *Mar. Pet. Geol.* 57, 470–481.
- Gallagher, S.J., Fulthorpe, C.S., Bogus, K., Auer, G., Baranwal, S., Castañeda, I.S., Christensen, B.A., de Vleeschouwer, D., Franco, D.R., Groeneveld, J., Gurnis, M., Haller, C., He, Y., Henderiks, J., Himmler, T., Ishiwa, T., Iwatani, H., Jatiningrum, R. S., Kominz, M.A., Korpany, C.A., Lee, E.Y., Levin, E., Mamo, B.L., McGregor, H.V., McHugh, C.M., Petrick, B.F., Potts, D.C., Rastegar Lari, A., Renema, W., Reuning, L., Takayanagi, H., Zhang, W., 2017a. Expedition 356 summary. *Proc. Int. Ocean Discov. Progr.* 356, 1–43. <https://doi.org/10.14379/iocp.proc.356.101.2017>.
- Gallagher, S.J., Fulthorpe, C.S., Bogus, K., Auer, G., Baranwal, S., Castañeda, I.S., Christensen, B.A., de Vleeschouwer, D., Franco, D.R., Groeneveld, J., Gurnis, M., Haller, C., He, Y., Henderiks, J., Himmler, T., Ishiwa, T., Iwatani, H., Jatiningrum, R. S., Kominz, M.A., Korpany, C.A., Lee, E.Y., Levin, E., Mamo, B.L., McGregor, H.V., McHugh, C.M., Petrick, B.F., Potts, D.C., Rastegar Lari, A., Renema, W., Reuning, L., Takayanagi, H., Zhang, W., 2017b. Site U1464. *Proc. Int. Ocean Discov. Progr.* 356, 1–45. <https://doi.org/10.14379/iocp.proc.356.109.2017>.
- Gallagher, S.J., Auer, G., Brierley, C., Fulthorpe, C.S., Hall, R., 2024. Cenozoic history of the Indonesian Gateway. *Annu. Rev. Earth Planet. Sci.* 52. <https://doi.org/10.1146/annurev-earth-040722-111322>.
- Goktas, P., Austin Jr., J.A., Fulthorpe, C.S., Gallagher, S.J., 2016. Morphologies and depositional/erosional controls on evolution of Pliocene–Pleistocene carbonate platforms: Northern Carnarvon Basin, Northwest Shelf of Australia. *Cont. Shelf Res.* 124, 63–82.
- Gortler, J.D., Rexilius, J.P., Powell, S.L., Bayford, S.W., Keep, M., Moss, S.J., 2002. Late early to mid-Miocene patch reefs, Ashmore Platform, Timor sea; evidence from 2D and 3D seismic surveys and petroleum exploration wells. *The sedimentary basins of Western Australia* 3, 355–376.
- Groeneveld, J., Henderiks, J., Renema, W., McHugh, C.M., De Vleeschouwer, D., Christensen, B.A., Fulthorpe, C.S., Reuning, L., Gallagher, S.J., Bogus, K., Auer, G., Ishiwa, T., Expedition 356 Scientists, 2017. Australian shelf sediments reveal shifts in Miocene Southern Hemisphere westerlies. *Sci. Adv.* 3, e1602567.
- Groeneveld, J., De Vleeschouwer, D., McCaffrey, J., Gallagher, S.J., 2021. Dating the northwest shelf of Australia since the Pliocene. *Geochem. Geophys. Geosyst.* 22, e2020GC009418. <https://doi.org/10.1029/2020GC009418>.
- Gurnis, M., Kominz, M., Gallagher, S.J., 2020. Reversible subsidence on the North West Shelf of Australia. *Earth Planet. Sci. Lett.* 534, 116070.
- Harrison, G.W.M., Santodomingo, N., Johnson, K.G., Renema, W., 2023. Is the Coral Triangle's future shown in a Pliocene reef gap? *Coral Reefs*. <https://doi.org/10.1007/s00338-023-02412-5>.
- Heath, R.S., Aporthe, M.C., 1984. New formation names for the late cretaceous and Tertiary sequence of the southern North West Shelf. *Geol. Surv. West. Aust. Rec.* 1984 (7), 1–35.
- Hengesh, J.V., Whitney, B.B., 2016. Transcurrent reactivation of Australia's western passive margin: an example of intraplate deformation from the central Indo-Australian plate. *Tectonics* 35 (5), 1066–1089.
- Herbert, T.D., Lawrence, K.T., Tzanova, A., Peterson, L.C., Caballero-Gill, R., Kelly, C.S., 2016. Late Miocene global cooling and the rise of modern ecosystems. *Nat. Geosci.* 9, 843–847. <https://doi.org/10.1038/ngeo2813>.
- Hughes, T.P., Barnes, M.L., Bellwood, D.R., Cinner, J.E., Cumming, G.S., Jackson, J.B., Kleypas, J., Van De Leemput, I.A., Lough, J.M., Morrison, T.H., Palumbi, S.R., 2017. Coral reefs in the Anthropocene. *Nature* 546 (7656), 82–90.
- Hull, J.N.F., Griffiths, C.M., 2002. Sequence stratigraphic evolution of the Albian to recent section of the Dampier Sub-Basin, North West Shelf, Australia. In: *Sedimentary Basins of Western Australia: Proceedings of Petroleum Exploration Society of Australia Symposium*, pp. 617–639.
- Hull, J.N.F., Smith, S.A., Young, H., 1998. Sequence Stratigraphic Interpretation of Carbonate Wireline Log Motifs: an example from the Northwest Shelf of Australia. *APPEA J.* 38, 188–198.
- Hunt, D., Fitch, W.M., 1999. Compaction and the dynamics of carbonate-platform development: Insights from the Permian Delaware and Midland basins, Southeast New Mexico and West Texas, USA. In: Harris, P.M., Saller, A.H., Simo, J.A. (Eds.), *Advances in Carbonate Sequence Stratigraphy: Application to Reservoirs, Outcrops and Models*, SEPMP Special Publication No. 63, pp. 75–106.
- Jones, H.A., 1973. Marine geology of the northwestern Australian continental shelf. *Bull. Bur. Mineral Resour. Geol. Geophys.* 136.
- Jones, L.A., Mannion, P.D., Farnsworth, A., Bragg, F., Lunt, D.J., 2022. Climatic and tectonic drivers shaped the tropical distribution of coral reefs. *Nat. Commun.* 13 (1), 3120.
- Karas, C., Nürnberg, D., Gupta, A.K., Tiedemann, R., Mohan, K., Bickert, T., 2009. Mid-Pliocene climate change amplified by a switch in Indonesian subsurface throughflow. *Nat. Geosci.* 2, 434–438.
- Karas, C., Nürnberg, D., Tiedemann, R., Garbe-Schönberg, D., 2011. Pliocene Indonesian Throughflow and Leeuwin current dynamics: implications for Indian Ocean polar heat flux. *Paleoceanography* 26 (2).
- Karatsolis, B.T., De Vleeschouwer, D., Groeneveld, J., Christensen, B., Henderiks, J., 2020. The late Miocene to early Pliocene “humid interval” on the NW Australian Shelf: disentangling climate forcing from regional basin evolution. *Paleoceanogr. Paleoclimatol.* 35 (9), e2019PA003780.
- Keep, M., Harrowfield, M., Crowe, W., 2007. The Neogene tectonic history of the North West Shelf, Australia. *Explor. Geophys.* 38 (3), 151–174.
- Keep, M., Holbourn, A., Kuhnt, W., Gallagher, S., 2018. Progressive Western Australia collision with Asia: implications for regional orography, oceanography, climate and marine biota. *J. Roy. Soc. West. Aust.* 101, 1–16.
- Kim, W., Fouke, B.W., Petter, A.L., Quinn, T.M., Kerans, C., Taylor, F., 2012. Sea-level rise, depth-dependent carbonate sedimentation and the paradox of drowned platforms. *Sedimentology* 59 (6), 1677–1694.
- Kleypas, J.A., Buddemeier, R.W., Gattuso, J.P., 2001. The future of coral reefs in an age of global change. *Int. J. Earth Sci.* 90, 426–437.
- Kuhnt, W., Holbourn, A., Schönfeld, J., Lindhorst, K., Gallagher, S., Keep, M., Sadekov, A., Dunlea, A., Clemens, S., Wilkens, R., Sarnthein, M., 2018. Cruise Report Sonne 257 [SO257], WACHEIO-Western Australian Climate History from Eastern Indian Ocean Sediment Archives, Darwin-Fremantle, May 12, 2017–June 04, 2017.
- McCaffrey, J., Wallace, M.W., Gallagher, S.J., 2020. A Cenozoic Great Barrier Reef on Australia's North West Shelf. *Glob. Planet. Chang.* 184, 1030148. <https://doi.org/10.1016/j.gloplacha.2019.103048>.
- Miller, K.G., Browning, J.V., Schmelz, W.J., Kopp, R.E., Mountain, G.S., Wright, J.D., 2020. Cenozoic Sea-level and cryospheric evolution from deep-sea geochemical and continental margin records. *Sci. Adv.* 6 (20), eaaz1346.
- Mitchum Jr., R.M., Vail, P.R., Sangree, J.B., 1977. Seismic stratigraphy and global changes of sea level, part 6: stratigraphic interpretation of seismic reflection patterns in depositional sequences. *Seism. Stratigr. Appl. Hydrocarb. Explor.* 165, 117–134. <https://doi.org/10.1038/272400a0>.

- Moss, G.D., Cathro, D.L., Austin Jr., J.A., 2004. Sequence biostratigraphy of prograding clinoforms, northern Carnarvon Basin, Western Australia: a proxy for variations in Oligocene to Pliocene global sea level? *Palaios* 19, 206–226.
- Pattiaratchi, C., 2006. Surface and sub-surface circulation and water masses off Western Australia. *Bull. Aust. Meteorol. Oceanogr. Soc.* 19 (5), 95–104.
- Perrin, C., Kiessling, W., 2012. Latitudinal trends in Cenozoic reef patterns and their relationship to climate. In: *Carbonate Systems during the Oligocene–Miocene Climatic Transition*, pp. 17–33.
- Petrick, B., Reuning, L., Auderset, A., Pfeiffer, M., Auer, G., Schwark, L., 2024a. High Sea surface temperatures were a prerequisite for the development and expansion of the Great Barrier Reef. *Sci. Adv.* 10, eado2058. <https://doi.org/10.1126/sciadv.ado2058>.
- Petrick, B.F., Reuning, L., Pfeiffer, M., Auer, G., Schwark, L., 2024b. Impact of the Late Miocene Cooling on the loss of coral reefs in the Central Indo-Pacific. *Clim. Past Discuss.*, in press. <https://doi.org/10.5194/cp-2024-28>.
- Prélat, A., Pankhania, S.S., Jackson, C.A.-L., Hodgson, D.M., 2015. Slope gradient and lithology as controls on the initiation of submarine slope gullies; Insights from the North Carnarvon Basin, Offshore NW Australia. *Sediment. Geol.* 329, 12–17.
- Purcell, P., Longley, I., 2023. The North West Shelf, Western Australia's super basin, in the twenty-first century. *AAPG Bull.* 107 (8), 1299–1367.
- Rankey, E.C., 2017. Seismic architecture and seismic geomorphology of heterozoan carbonates: Eocene-Oligocene, Browse Basin, Northwest Shelf, Australia. *Mar. Pet. Geol.* 82, 424–443.
- Riera, R., Bourget, J., Allan, T., Håkansson, E., Wilson, M.E., 2022. Early Miocene carbonate ramp development in a warm ocean, North West Shelf, Australia. *Sedimentology* 69 (1), 219–253.
- Riera, R., Paumard, V., Bourget, J., Allan, T., Lebruc, U., 2023. Evolution of the Exmouth-Barrow carbonate margin through the Miocene: Insights from 3D seismic data and field investigations (North West Shelf, Australia). *Sediment. Geol.* 449, 106371.
- Rohling, E.J., Yu, J., Heslop, D., Foster, G.L., Opdyke, B., Roberts, A.P., 2021. Sea level and deep-sea temperature reconstructions suggest quasi-stable states and critical transitions over the past 40 million years. *Sci. Adv.* 7 (26), eabf5326.
- Romine, K.K., Durrant, J.M., Cathro, D.L., Bernardel, G., 1997. Petroleum play element predication for the Cretaceous-Tertiary basin phase, northern Carnarvon Basin. *APPEA J.* 37, 315–339.
- Rosleff-Soerensen, B., Reuning, L., Back, S., Kukla, P., 2012. Seismic geomorphology and growth architecture of a Miocene barrier reef, Browse Basin, NW-Australia. *Mar. Pet. Geol.* 29, 233–254.
- Rosleff-Soerensen, B., Reuning, L., Back, S., Kukla, P.A., 2016. The response of a basin-scale Miocene barrier reef system to long-term, strong subsidence on a passive continental margin, Barcoo Sub-basin, Australian North West Shelf. *Basin Res.* 28, 103–123.
- Ryan, G.J., Bernardel, G., Kennard, J.M., Jones, A.T., Logan, G.A., Rollet, N., 2009. A precursor extensive Miocene reef system to the Rowley Shoals reefs, WA: evidence for structural control of reef growth or natural hydrocarbon seepage. *APPEA J.* 49, 337–363.
- Salzmann, U., Williams, M., Haywood, A.M., Johnson, A.L., Kender, S., Zalasiewicz, J., 2011. Climate and environment of a Pliocene warm world. *Palaeogeogr. Palaeoclimatol. Palaeoecol.* 309 (1–2), 1–8.
- Sanchez, C.M., Fulthorpe, C.S., Steel, R.J., 2012. Middle Miocene–Pliocene siliciclastic influx across a carbonate shelf and influence of deltaic sedimentation on shelf construction, Northern Carnarvon Basin, Northwest Shelf of Australia. *Basin Res.* 24, 664–682.
- Saqab, M.M., Bourget, J., 2016. Seismic geomorphology and evolution of early–mid Miocene isolated carbonate build-ups in the Timor Sea, North West Shelf of Australia. *Mar. Geol.* 379, 224–245. <https://doi.org/10.1016/j.margeo.2016.06.007>.
- Schlager, W., 1981. The paradox of drowned reefs and carbonate platforms. *Geol. Soc. Am. Bull.* 92 (4), 197–211.
- Smith, S.A., Tingate, P.R., Griffiths, C.M., Hull, J.N.F., 1999. The structural development and petroleum potential of the Roebuck Basin. *APPEA J.* 39 (1), 364–385.
- Smith, R.A., Castañeda, I.S., Groeneveld, J., De Vleeschouwer, D., Henderiks, J., Christensen, B.A., Renema, W., Auer, G., Bogus, K., Gallagher, S.J., Fulthorpe, C.S., 2020. Plio-Pleistocene Indonesian throughflow variability Drove Eastern Indian Ocean Sea surface temperatures. *Paleoceanogr. Paleoclimatol.* 35 (10), e2020PA003872.
- Steinhorsdottir, M., Coxall, H.K., De Boer, A.M., Huber, M., Barbolini, N., Bradshaw, C. D., Burls, N.J., Feakins, S.J., Gasson, E., Henderiks, J., Holbourn, A.E., 2021. The Miocene: the future of the past. *Paleoceanogr. Paleoclimatol.* 36 (4), e2020PA004037.
- Tagliaro, G., Fulthorpe, C., Gallagher, S., McHugh, C., Kominz, M., Lavier, L., 2018. Neogene siliciclastic deposition and climate variability on a carbonate margin: Australian Northwest Shelf. *Mar. Geol.* 403, 285–300.
- Tesch, P., Reece, R.S., Pope, M.C., Markello, J.R., 2018. Quantification of architectural variability and controls in an Upper Oligocene to lower Miocene carbonate ramp, Browse Basin, Australia. *Mar. Pet. Geol.* 91, 432–454.
- Thronberens, S., Back, S., Bourget, J., Allan, T., Reuning, L., 2022. 3-D seismic chronostratigraphy of reefs and drifts in the Browse Basin, NW Australia. *Bulletin* 134 (11–12), 3155–3175.
- Van Tuyl, J., Alves, T.M., Cherns, L., 2018a. Geometric and depositional responses of carbonate build-ups to Miocene Sea level and regional tectonics offshore Northwest Australia. *Mar. Pet. Geol.* <https://doi.org/10.1016/j.margeo.2018.02.034>.
- Van Tuyl, J., Alves, T.M., Cherns, L., 2018b. Pinnacle features at the base of isolated carbonate buildups marking point sources of fluid offshore Northwest Australia. *Geol. Soc. Am. Bull.* 130, 1596–1614.
- Wallace, M.W., Condilis, E., Powell, A., Redfearn, J., Auld, K., Wiltshire, M., Holdgate, G. R., Gallagher, S.J., 2003. Geological controls on sonic velocity in the Cenozoic carbonates of the Northern Carnarvon Basin, North West Shelf, Western Australia. *APPEA J.* 43, 385–399.
- Westerhold, T., Marwan, N., Drury, A.J., Liebrand, D., Agnini, C., Anagnostou, E., Barnett, J.S., Bohaty, S.M., De Vleeschouwer, D., Florindo, F., Frederichs, T., 2020. An astronomically dated record of Earth's climate and its predictability over the last 66 million years. *Science* 369 (6509), 1383–1387.
- Williams, C., Paumard, V., Webster, J.M., Leonard, J., Salles, T., O'Leary, M., Lang, S., 2023. Environmental controls on the resilience of Scott Reefs since the Miocene (North West Shelf, Australia): Insights from 3D seismic data. *Mar. Pet. Geol.* 151, 106188.
- Wilson, S.K., Depczynski, M., Fisher, R., Holmes, T.H., O'Leary, R.A., Tinkler, P., 2010. Habitat associations of juvenile fish at Ningaloo Reef, Western Australia: the importance of coral and algae. *PLoS One* 5 (12), e15185.
- Woodroffe, C.D., Webster, J.M., 2014. Coral reefs and sea-level change. *Mar. Geol.* 352, 248–267.
- Young, H.C., Lemon, N.M., Hull, J.N.F., 2001. The Middle Cretaceous to recent sequence stratigraphic evolution of the Exmouth-Barrow margin, Western Australia. *APPEA J.* 41, 381–413.